SAND80-1455/II

SEISMIC REFLECTION MAPPING OF DISCONTINUOUS SANDSTONE BODIES

PART II - FIELD EXPERIMENT

T. L. DOBECKI

Sandia National Laboratories

SF 2900-Q(3-80)

Issued by Sandia Laboratories, operated for the United States Department of Energy by Sandia Corporation.

SF 1004-DF(11-77)

Printed in the United States of America

Available from National Technical Information Service
U.S. Dept. of Commerce
5285 Port Royal Road
Springfield, VA 22161

Price: Printed Copy: $5.50
Microfiche:' $3.00

TABLE OF CONTENTS

SAND80-1455/II

SEISMIC REFLECTION MAPPING OF DISCONTINUOUS SANDSTONE BODIES

PART II
FIELD EXPERIMENT

T. L. Dobecki
Sandia National Laboratories
Albuquerque, NM 87185

ABSTRACT

Three-dimensional seismic reflection data were acquired at a site in East-Central Utah where known sandstone channeling existed in the O-1500 ft depth range. The site was atop a bluff-bounded on three sides by cliff faces on which the channels were observed to outcrop. Geologic descriptions of outcrop and a corehole were developed in coordination with this seismic investigation as a means of evaluating the seismic interpretation.

Two-dimensional vertical slices of the 3-D data exhibit characteristics similar to those observed in a companion synthetic model study of channel sands. Observed reflections were discontinuous, exhibited channel character (concave-convex surfaces, peak-to-peak thickening), and could be correlated on a number of parallel sections. Two-dimensional horizontal (time) slices of these same data support the interpreted trend and attitude of three channels as determined from the vertical sections. When projected from the area of the seismic survey out to outcrop position on the cliff face, these seismically determined channels have a good correlation with observed, outcropping sandstones. Disagreement between seismically predicted channel trend and trend determined statistically from outcrop measurements exists, but for two of the three channels detected, this disagreement is minor.

1.0 INTRODUCTION

Part I of this report (Dobecki, 1980) outlines the rationale behind employing seismic techniques for the mapping of sandstone channel reservoirs typical of the tight (low permeability) gas sands of the Western United States. That report also characterizes the theoretical seismic signature of such channel bodies by way of a two-dimensional synthetic seismogram study.

This section Of the report, Part II - Field Experiment, describes a coordinated field program employing combined seismic, borehole, and outcrop information to evaluate the effectiveness of seismic techniques in mapping actual channel sands.

A site was chosen which exhibited shallow (o-2000 ft depth) channels, some underlying continuous horizons, and extensive outcrop information. A three-dimensional seismic survey was performed at this site in December, 1979 through early January, 1980. This report presents the results of this survey and a seismic interpretation based upon input from the synthetic models, outcrop, and well log data.

2.0 SITE DESCRIPTION

The primary requisites for a site suitable for performance and evaluation of such a seismic experiment may be listed as follows.

1) Depth to channeling should be relatively shallow (less than 4,000 ft). Reflections from shallower targets should retain more higher frequency components in the seismic wavelet and thereby optimize the seismic passband as suggested by the model study described in Part I of this report.

2) The target section should contain known channeling. The area should have sufficient control to know that channels exist and what range of sizes and distribution with depth might be expected.

Such a site was located in the Bryson Canyon Gas Field of east-central Utah. Location of the site was determined with the help of William B. Cashion

(U.S.G.S.) and Carroll F. Knutson (C.K. Geoenergy Corp.). Dr. Cashion has had extensive experience in mapping the geology of the Uinta Basin, and Dr. Knutson is under DOE contract to develop a means of predicting channel behavior by means of corehole and outcrop analysis of sedimentary structures contained in channels. It was decided that it would therefore be best to coordinate the seismic and corehole/outcrop programs and perform these together at a site meeting the requirements of both.

The site is physically located in east-central Utah (Figure 1) near the Colorado border, some 50 miles northwest of Grand Junction, Colorado. The location is generally known as the East Canyon area, Specifically, the site occupies a flat topped ridge (Figure 2) in Section 16, T17S, R24E in Grand County, Utah. The area where the seismic survey and corehole were placed was the top of the flat ridge within the rectangle drawn on Figure 2. The ridge is bounded on three sides by steep cliffs exposing nearly 1110 ft of the subsurface in their faces.

Geologically, the site is located near the southeast edge of the Uinta Basin. The top of the ridge (Figure 3) in the seismic survey area, consists of the Tuscher Fm. (part of the upper Cretaceous Mesa Verde group) with underlying Farrer and Neslen formations (also Mesa Verde) exposed in the cliff faces. Significant channel development is observed in the Farrer with fewer channels seen in both the overlying Tuscher and underlying, coal bearing Neslen. Deeper formations, exposed in outcrop on the drive into the site but not in the cliff faces, include the blanket Sego sand, the Buck Tongue of the Mancos shale, the blanket Castlegate sand, and the Mancos shale. Vertically beneath the site, then, is a section of approximately 1500 ft of sands having channeling underlain by a thick section of continuous beds. In addition to the information provided by the planned C. K. Geoenergy corehole (GC #1), the site physiography itself presents an unique input to the seismic program in that most of the objective section (upper 1500 ft) is exposed on the cliff faces.

The site is also affected by local structure as it is situated on the

southern flank of the Westwater anticline. This feature trends roughly east-west and plunges to the west. The Bryson Canyon field and the Westwater gas field farther west are located on the crest of the anticline but produce from deeper formations than the Mesa Verde group, The effect on the seismic site area is to introduce dip to the south and west which will be superimposed on the trend of the channels. A minor amount of faulting is observed in the area as seen on a geologic map of the region (Cashion, 1973), and, in the course of his detailed outcrop study of the ridge, Dr. Knutson encountered only one, minor east-west fault (Knutson, personal communication).

The area of the site is under' the control of the Bureau of Land Management (BLM) and therefore all plans for drilling, clearing, and performance of the seismic survey were submitted to and approved by the BLM office in Moab, Utah.

3.0 SEISMIC SURVEY

3.1 Input geologic and well log data. From the outcrop study by Knutson (personal communication), it was apparent that most channeling could be expected in the Farrer fm. and that typical size would range from a few up to 60 ft in thickness and, typically, 150-200 ft in cross-sectional width. Well GC #1 was drilled at about the same time as the seismic data were obtained. It reached a total depth of about 1,050 ft and was logged. The logs run included: Borehole Compensated Sonic (BHC), Caliper, Natural Gamma, and Four-arm Continuous Dipmeter. Figure 4 presents a portion of the BHC-Gamma log. Most apparent from this section is the fact that the sands (noted by dotting on gamma log), particularly 280-304 ft, 385-410 ft, and 434-474 ft (called the "Green" channel in this report) are lower velocity (8,000-8,700 ft/s) than the shalier background material (10,000-10,600 ft/s). This is in contrast with observed velocities deeper in the Uinta Basin (V_{Sand} = 11,800 ft/s) and as used in the modeling program. This is felt due both to fracturing observed in the channels in outcrop and to leaching of cement by groundwater flow in the sands at these shallow depths. However, the contrast in

velocity across channel boundaries remains so reflections, albeit of opposite polarity than modeled, should still be generated by the channels.

The sonic log was digitized, and a one-dimensional synthetic seismogram was generated by Seismic International Research Corporation (SIRC), the contractor chosen to perform the seismic survey. This seismogram (Figure 5) starts with T = 0.000 sec equivalent to the top of the log (160 ft depth), therefore a time error representing two-way reflection time from the surface to 160 ft is present. This was eliminated, however, by shooting into a geophone at a known depth placed in the well for a true time tie. This time correction is measured at +47 milliseconds. Several obvious features on the seismogram are immediately apparent. First, the effect of the three thicker channels (including the "Green" channel) in the upper 500 ft of the log is characterized by a separate event for the shallowest but a composite event for the lower two. That is, the channel reflection from the 385-410 ft overlaps the "Green" channel reflection because the two bodies are only 24 ft apart. The "Green" reflector is arbitrarily given this name as green is the color used to follow this event in the interpretive phase described later. The response of the Green reflector, then, is characterized by the segment of the composite event as indicated on Figure 5. Therefore, any channeling involving this reflector will be characterized by trough-to-trough thickening of this "Green" composite. A second observation, given noise free data, is that the coal bed near 924 ft (within the Neslen fm.) should provide a large amplitude and continuous (when compared with channel deposits) reflection.

The log data and the derived synthetic record show that a) several discrete sand beds exist, and these are assumed to be channels as no continuous type of sand bed is observed in outcrop, b) the velocity contrast shown by the channels yields good reflections, and c) the response of channels separated by only 20 ft overlap in time yield a composite reflection.

3.2 Field procedures and initial observations. The seismic program was a 3-D, or areal, seismic survey. This means that instead of a number of

explosive shot points, for example, being recorded by a linear array of receiver (geophone) stations, a number of shot points are recorded by a two-dimensional array of geophone stations. Figure 6 shows, basically, the field arrangement employed in this field data acquisition program. A rectangular array of geophone stations (6 stations by 8 stations) was set out while 6 shot points were fired. Each shotpoint, then, generated a separate record of 48 channels. By shooting in this fashion and then moving the whole array along the direction of traverse, a dense array of common depth points (CDP's) are developed. Running additional, overlapping traverses results in complete coverage of an area. Figure 7 shows the net CDP covered area at the survey site. The area is approximately 750 ft x 1,080 ft and includes the location of well GC #1. CDP spacing is 15 ft, yielding a 50 x 72 grid of subsurface data points or a total of 3,600 CDP's.

Figure 8 shows two raw displays of shot data; each display shows the output from a 48-geophone rectangle for a single shot. Each shot source was a length (5 ft) of primacord; recording was made by SIRC using a 48-channel digital seismograph. It is apparent that the air wave from the shot is a major source of noise, leaving a narrow time window in which to record reflections. This is a common problem in shallow seismic surveying; the travel time for the target reflections is very close to the travel times of shot generated noise. In this respect, this particular survey might have been simpler if the objectives were actually deeper. However, promising alignments before the air wave arrival indicate the presence of valid reflections.

In addition to the sonic log, a time calibration was obtained by shooting from the surface into a geophone located at a depth of 260 ft in well GC #1. Recorded time was 0.036 sec or a reflection time of 0.072 sec for a 260 ft depth. This corresponds to the earlier mentioned time tie of 0.0465 sec for the synthetic seismogram.

4.0 PROCESSED RESULTS AND INTERPRETATION

Basically, there are three possible ways to display three-dimensional (X, Y, T) seismic data. The entire data set may be displayed, but this requires a three-dimensional display format which must also be transparent to display internal data points. This, although instructive, would be cumbersome and difficult to manipulate, A second possibility would be to display the data on selected vertical planes, or vertical slices. For example, the plane (X, 0, T) represents a normal-type seismic record section (X, T) along a line Y = 0. Any arbitrary slice of the data will produce a time section. This enables the interpreter to select dip lines, strike lines, etc. by merely selecting lines in those directions. The third possibility would be to display the data on selected horizontal planes, or time slices. This is a relatively new method of display and unfamiliar to even most geophysicists used to working with seismic data. For example, the plane (X, Y, Tl) represents a map of reflection amplitude values over the entire survey area (X, Y) at a given value of reflection time, T_1. As this is a map of amplitudes, each data point (CDP) has an amplitude represented by a gray scale (or color) where black represents maximum positive amplitude (peak) and white is minimum (trough). Therefore, a horizontal reflector will be a uniform shade at its time of reflection. Dipping and curved reflections will be represented by bands on dark and light having very much the same appearance as an outcrop pattern on a geologic map. Figure 9 shows some simple block diagrams of 3-D structural (not seismic) situations, although the extension to seismic should be obvious. The sides of each block represent vertical slices while the tops and bottoms correspond to time slices.

In the following, a series of vertical slices will be discussed and interpreted in terms of channeling. These will be followed by a series of time slices, and any correspondence between the two displays will be noted.

4.1 Vertical slice display. Refering to Figure 7, it is noted that the rectangular area shows six columns labeled "T-l" through "T-6." These six

traverses represent the six vertical slices presented in this section. A single slice section is presented for each traverse although each is a weighted combination of twelve possible, parallel slices within each traverse. The maximum CDP "fold", or data redundancy, of each presented section is 120 which is very substantial. Well GC #1 falls along traverse 3, so this is the logical section with which to begin analysis. Figure 10 shows an uninterpreted segment of the section along traverse 3 with the synthetic seismogram superimposed at the approximate position of well GC #1. Note that each (section and synthetic) is plotted in reverse polarity (actual peaks become troughs and vice versa). From the model study of Part I which had the reverse velocity situation (higher velocity channels) peak-to-peak thickening (trough widening) was a characteristic of channeling. By plotting reverse polarity, the field data has the same character as the models. Particular items to notice on the match is a) the "Green" reflection (labeled "G") on figure 10 is easily seen, b) the shallower, sand reflection is lost in early shot noise, and c) the coal reflection is poorly reproduced. The loss of the coal reflection is due to its arrival at nearly the same time as the air wave interference. It is apparent that the coal reflection will not be usable under these circumstances: therefore one criterion noted in the model study, disruption of underlying continuous reflections, is not available as an interpretive tool in this study. I will now proceed to present traverse section 1 through 6 concentrating primarily on the "Green" reflector but noting other features on the sections. It is important to recall at this time that we are dealing with reflectors known to be discontinuous. Disruptions of a signature most likely represent actual discontinities; i.e., even if a reflection continues (apparently) beyond a disruption it is more than likely the response of a different sand body. Given the guidelines for detecting a channel seismically, as determined in the Part I model study, interpretations of the six vertical slices are given in the following.

4.1.1 Traverse 3. As stated previously, this traverse intersects the well

GC #1 and is the obvious starting point for an interpretation. If particular channel events can be noted on this section, especially if they can be tied to the well, the next step would be to move to adjacent sections to see if these same events persist laterally. In this way, the whole area may be mapped.

Figure 11a is the processed, although uninterpreted, section along traverse 3. On the whole, this section exhibits several reflections; however, there are no reflections which are continuous across the entire section. The only ways a continuous reflector would be seen are a) if continuous beds existed or b) if the traverse paralleled the channel axis. The first is not valid until several thousand feet deeper, and the second would require a good deal of luck. The discontinuous nature of the reflections is simply a consequence of the geology. Figure 11b shows the same section interpreted in terms of channeling. The reflections so marked signify the "Green" reflector at the well position (marked C on figure) and other, unknown bodies away from the well. This interpretation was made as follows. The vertical lines were marked on the record at positions where a seemingly continuous set of reflections terminated. The peaks above and below the "Green" trough were traced outward from the well and continued across a discontinuity if the offset in reflection time was slight. Across major discontinuities (e.g. at CDP #335) another, arbitrarily chosen interval was also marked off. To be considered a channel reflection, the reflection should be flat or convex on its upper surface, flat or concave *on* its lower surface, should show peak-to-peak thickness variation, amplitude increase on the *lower* reflection, and be discontinuous in most cases. Section 3, therefore, might possibly be interpreted as showing the responses of four sand channels as separated by the vertical lines on figure 11b. CDP 335 definitely separates two bodies as there is substantial offset (20 milliseconds) of the reflections on either side. To the left of CDP 335, the channel, if I may use the term, is substantially deeper, on the order of 100 ft, than the channel to the right.

It, as well as the reflection outlined to the right of CDP 335, exhibits the peak-to-peak thickening as well as a divergent upper reflection. The divergence is minimal, however, due to the presence of noise on the section and to the observation of only slight curvature on most lenses as seen in outcrop.

To the right of CDP 335, we have a choice of interpretations. Either three separate but closely spaced channels, exist at approximately the same depth, two channels (separated near CDP 320) , or one large channel faulted near CDP 320. As little faulting has been observed in outcrop, the tendency is to consider two channels. Minimum widths of these channels which, for convenience, I will lable A, B, and C (figure llb), C being the "Green" sand of well GC #1, are A = 180 ft, B = 150 ft, and C = 285 ft. Both channels A and C continue off the section, therefore their widths are given as minimum. Separate top and bottom reflections are not observed, so channel thicknesses must be less than 0.5 wavelength. One wavelength, given the velocity and approximate central frequency of the wavelet, is on the order of 130'. Given thickness in GC #1 of the "Green" sand as 40 ft (80 ft if the smaller sand above it is included), we can estimate that each channel seen is on the order of 40 ft thick.

The test of whether or not these are real expressions of channels is how well these same features correlate with observations on other traverses. I will proceed first to the east of traverse 3 (to numbers 2 and 1) then, afterwards, to the west (numbers 4, 5, and 6).

4.1.2 Traverse 2. The first and most striking observation made in looking at Section 2 (figure 12a) is the higher level of noise as evidenced by the poorer signal amplitude and coherency, However, by following the same interpretive procedure as described for traverse 3, and also by overlaying 2 on 3, it is obvious that similar events can be interpreted on section 2 (figure 12b). The same three channels are seen, as judged by width and event character. The most significant difference is with "A" channel which on section 2 appears distorted, perhaps thicker, although in proper depth relationship to the other

channels. It is felt this may be due to interference from the response of another nearby channel not present at this position on section 3. This is based in part on the interpretation of section 1, so additional input will be made in the following section. The shapes and positions of the channels are very similar to section 3 which instills confidence in the interpretation of these as discrete, real bodies.

4.1.3 Traverse 1. Section 1 (figure 13a) is an improved section compared to 2 with a higher signal to noise ratio (S/N). The reflections, although discontinuous, are much clearer and easier to follow. The interpreted section (figure 13b) shows, again, the same three channels, but their positions have moved slightly north (right). We can see the full width of "A" (240 ft) as it appears totally on the section. A striking observation is the appearance a new event labeled E on the section. This is the most convincing "channel" signature that is seen on any section in this report. It exhibits all the characteristics (convex-concave reflections, thickening) expected from the Part I model study. It is some 300 ft deeper than channel B and is thicker. However, it is not observed on section 3 or in well GC #1. This implies the channel must trend a different direction than A, B, or C. We also note that A has the same, non-interference, shape on section 1 as on section 3. It is felt that channel E is the interfering channel mentioned in the previous traverse description; the trend of channel E could be such that it is quite close to A on section 2. Also, no other manifestation of E is seen on section 2 apart from the interference at A. If correct, this implies that channels A, B, and C, to this point are nearly parallel features, but deeper channel E is trending in a substantially different direction. This is an important observation in terms of the objectives of this experiment; that is, channel trend may vary with depth.

Another important observation is that going from traverse 3 to 1, the events have occurred sooner, or at earlier times. This means there is a component of dip up from 3 to 1 which is to the northeast. This is consistent

with the local structural situation described earlier. The site is on the south flank of a westward plunging anticline; structural dip should be down to the southwest, or up to the northeast. Realize, however, that this is post-depositional structure and had no bearing on the orientation of the channels when they were actively forming as river beds.

4.1.4 Traverse 4. This section (figure 14a) also shows good signal to noise ratio (S/N). The interpretation, shown on figure 14b, again shows the same channels. In this instance, however, channels B and C show a more definite separation than on traverse 3, which implies that although quite close to one another, they are apparently separate bodies.

4.1.5 Traverse 5. This section (figure 15a) much like traverse 2 has poor S/N, but using the same procedures as before, an interpretation can be made which is consistent with the developing subsurface situation. The three channels maintain their typical positions with C separate from B. The shapes of the events, however, are quite distorted felt due primarily to the increased noise on this section. It appears that the left limit of A is just into the section, the width implied being the same as interpreted from traverse 1.

At this point it is worth discussing probable sources of noise which seems to vary in intensity across the site. The site of the survey itself rests on outcropping Tuscher formation which consists of some very large, almost continuous-looking channel sands. Therefore, right at the surface is a hard sandstone which under normal circumstances would be expected to ring under application of an impulsive stress load. In most shots, looking at unprocessed shot point records such as figure 8, we see that this was not the case. However, due to source coupling, characteristics of the sand, or other unknown reasons, significant ringing was occasionally encountered. This is the suspected culprit which caused signal degradation along Traverses 2 and 5.

4.1.6 Traverse 6. This final two-dimensional record section is the south-western-most in the survey area. The uninterpreted section (figure 16a)

shows increased S/N compared to section 5 but still below that of section 3. The interpreted section (figure 16b) is quite similar to that of section 3 with channel C overlapping the channel B response. Reflection times to all events are later than section 3 by some17 milliseconds, again attesting to the SW structural dip in the area. This dip provided no indication as to direction of channel flow as we know flow was generally toward the ancient sea which was to the east of the land mass. The general apparent structural dip (in terms of reflection time) across the site area there is approximately 33 milliseconds per 1,000 ft (two-way time). This number will prove useful when projecting seismically observed channels to their predicted outcrop positions.

4.1.7 Summary of two-dimensional sections. We have seen that a set of discrete reflection events having the characteristics of channels have been observed consistently across the survey area. Three of these are essentially parallel with a fourth, deeper and non-parallel event observed on only two sections. To interpret these in terms of channel trend, I have plotted (figure 17) the interpreted channel edges for A, B, and C on the map of seismic control. The channels meander about an average trend of N 60° E as shown on the map view. Note that this is a projected map view - all three channels are at different depths, channel A particularly so. Also, the northeastern ends are shallower than the southwestern ends by an estimated 128 ft using an average velocity to the channels of 8,500 ft/s. Therefore, a true horizontal slice at a given depth would not show such a picture of three channels; rather it would show only the outcrop pattern of one or two of them. A similar projection of channel E would trend approximately N 10°E or at an angle of 50° from the trend of the shallower channels.

The next step in the analysis of these seismic data is the comparison of this two-dimensionally derived interpretation with' the analyzed three-dimensional data.

4.2 Three-dimensional, horizontal slice display. Before discussing the time slice data, some preliminary thoughts on what the data should look like are in order. If the channels were horizontal (i.e. no dip), then a single time slice through a channel would show the full pattern, or map, of that channel across the survey area. If the channel is dipping, however, several time slices are required; shallow depths at earlier times, deeper points at later time slices. Further, the pattern of a channel on any time slice will be a distorted view of a channel. To illustrate, figure 18 shows the outcrop pattern of a channel, of elliptical cross section, for dips of 0, 10, 45, and 90 degrees. The 90-degree case, the channel being vertical, is not an expected field reality, but its outcrop pattern shows the true cross-section of the channel. If the same channel is dipping, its outcrop elongates in the direction of dip: the more the dip, the greater the elongation. Further, if deeper horizontal slices are made, the pattern will progressively move down dip. Also, as the reflection response consists basically of a top peak, trough, and bottom peak, all three will be seen on a single time slice if the channel is diping. The bottom reflection will, of course, be observed at the updip end of the total channel reflection. The final case (0 degree dip) is the situation refered to earlier; the whole channel is observed on a single horizontal slice. If additional structure, such as faulting or warping, is superimposed upon this simple picture, the observed patterns could become quite complicated.

The time slice sections to be presented are positive polarity, or opposite the vertical slice sections, such that a trough on a section will be characterized by a dark point on the time slice while a peak becomes a white spot. Again, each CDP will be represented by a 15 ft x 15 ft square, or pixel, on the time slice. The amplitude of the received signal at a given CDP at a given time is represented by a grey scale (peak = white; trough = black). A priori, from the previous section, we know that the reflections are dipping. This means several different reflections will be observed on a single time

slice (see, for example, figure 9b). An important part of reducing such time slice data, then, includes determining which patterns observed belong to the same reflection. This will become apparent when observing real data examples.

Figure 19 is an example of an uninterpreted time slice at a two-way reflection time of 0.136 sec. The several patterns outlined have an apparently random orientation. However, some may represent the top and bottom reflections from the same reflector (because of dipping beds) while other patterns may represent totally different reflectors. Each pattern, then, must be identified with a given reflection event. To do this, we must go back and forth between vertical slices and horizontal slices and make consistent identifications. On the vertical sections, I identified three channels (A, B, and C) and associated a top peak and a bottom peak with each. I will maintain this same nomenclature by mapping only the top and bottom peaks ("white" areas) on the time slice data. The total range of reflection times is from 0.095 sec (top of B and C in NE corner) to 0.175 sec (bottom of A in SW corner). Four time slices at times of 0.116, 0.120, 0.124, and 0.128 sec are interpreted and shown on figure 20. These times cut through the heart of channels B and C and therefore should represent their trends very Well. The shallowest slice (T = 0.116) shows that for B and C the dip is toward the lower left and the pattern for each is generally elongate from left to right. The next deepest slice intersects the top and bottom reflections over a greater area, and the trend of the channels is more apparent. For comparison, the projected limits of channel B taken from vertical slice data (from figure 17) are superimposed on this time slice. Although displaced slightly towards the bottom of the figure, the reflection pattern follows the two-dimensional interpretation very well. On the third section, we observe that the deeper channel (A) is starting to contribute more to the picture, and that the shallower channel reflections are moving down dip and becoming less dominant. These observations continue onto the deepest slice shown here. The trends of channels A, B, and C, then, agree with the two-dimensional, vertical

section interpretation. The observation that the interpretations agree is not surprising as both represent different views Of the same data. However, taken alone, either set has some uncertainty in the validity of the interpretation; agreement between the two lends a great deal of confidence to the common interpretation.

The overall interpretation, then, is that there are a minimum of three channels which trend N 60° E across the seismic survey area in a depth range of approximately 400 - 700 ft. One channel, C, is intersected by borehole GC #1, and another, B, lies very close to C although slightly shallower. The third channel, A, lies farther south of B and C, (approximately 300' S of B) has nearly the same trend, but is some 80-100 ft deeper than B. The channels are typically 150 ft to 280 ft wide, on the order of 40 ft thick, and traverse the whole survey area (i.e. minimum length of 1,080 ft). An additional, questionable channel, called E, is observed on section 1 as a well developed event. However, it is not clearly seen on section 2, save for a distortion of channel A. If this can be assumed due to interference from E, then this channel trends N 10° E and lies some 180-200 ft below channel C in the area of traverse 1. If a valid channel, this would imply that channel orientation may change as a function of depth reflecting different fluvial conditions at varied depositional periods.

5.0 COMPARISON WITH COREHOLE AND OUTCROP GEOLOGY

A test of the accuracy of the interpretation of the seismic data is by comparison with geologic data available from corehole GC #1 and from the outcrop mapping performed by C. K. Geoenergy Corporation (CK).

CK geologists have measured the thickness and outcrop pattern of some 250 sandstone channels greater than 5 ft thick from the surface (Tuscher) down into the Neslen fm. at the bottom of the cliffs. Besides purely geometric descriptions, measurements of the channel trend were estimated using a statistical approach as described by Knutson (1978). The study utilizes numerous measurements of the orientations of primary structural elements

(e.g. trough cross beds) within a single channel outcrop to determine channel orientation. The only means of comparison of the two sets of data would be either to project the sand channels from outcrop back into the survey/well area or to project the seismic interpretation to outcrop. The latter might be more meaningful because the outcrop study gives instantaneous, or single point, orientation; that is, it gives flow direction at the outcrop position and not really the average channel direction. The seismic interpretation shows channel behavior over 1,080 ft and exhibits meandering behavior as well as average trend. Given this as the means for comparison, I shall attempt to project channels A, B, and C to their outcrop positions. As channel C intersects the well, it is the logical starting point.

Elevation of the top of channel C in GC #1 is given as 6,238 ft above MSL. To determine where it will intercept the cliff face we need to know its trend and its dip. The only measure of dip we have is in terms of reflection time. The average value used will be 33 ms per 1,000 ft. This translates to a dip along the channel axis of approximately 140 ft per 1,000 ft (8°). That means, at a range of 1,500 ft from the well along azimuth N 60° E, the top of channel C would be at an elevation of 6,425 ft. At a range of 900 ft from the well, it would be at an elevation of 6,350 ft. It turns out, using the topographic map of figure 2 and the N 60° E azimuth, the channel top should crop out at a range of 950 ft at an elevation of 6,370 ft. A similar treatment of channels A and B would not exactly be possible as they are not tied to the well. However, I can estimate their depths within traverse 3 by noting their reflection times. Such an analysis yields approximate elevations of the tops of A and B, respectively, as 6,075 ft and 6,190 ft at the middle of the channel and at the middle of traverse 3. Projecting the same dip and the same azimuth from these points, we find range and elevations of outcrop as (1,100 ft, 6,340 ft) for B and (1,200 ft, 6,240 ft) for A. On figure 21, a section of the topographic map, the starting points within the survey, and the vectors to the outcrop projections are all given. Also given on figure 21 are the outcrop

patterns of some sand channels which have been mapped by CK. The numbers next to each are identification numbers used by CK. Obviously, these are candidate channels actually observed which appear very near the projections of A, B, and C. The nearness to the projection as well as their close proximity to each other make channels 8 and 10 the most reasonable choice for C and B respectively, while channel 7 occurs closest to the projected outcrop of A. However, because of changing values of dip moving toward the crest of the Westwater anticline, it is possible that channels 4 and 5 could represent channels C and B. This uncertainty cannot be resolved. Measured and calculated parameters of channels 4, 5, 7, 8, and 10 are presented (Knutson, personal communication) along with the corresponding seismic determinations in Table I.

TABLE I Comparison of Seismic and Outcrop Descriptions of Channel Sandstones

Channel	Elevation (top)	Thickness	Width	Bearing
A	6,240	40 (?)	240	N 60° Et
7	6,240	8	?	N 25° E*
B	6,340	40 (?)	150	N 60° Et
10	6,400	20	240	N 100° E*
5	6,280	10	?	N 25° E*
C	6,370	40 (?)	285	N 60° Et
8	6,410-6,420	26'	375'	N 0°E*
4	6,310-6,320	25'	?	N 20° E*

t average bearing of meandering channel

* bearing of meander based on single point

Note from the comparison that the most glaring discrepancy lies in the channel bearing. This is due, as mentioned previously, to comparing average channel trend with a single point trend, or trend of a meander section. From both the

two dimensional map projection (Figure 17) and the time slice data (figure 20), we can easily observe that the channel patterns are not straight, but do meander. The N 60" E is the average bearing, but, on channel C for example, the bearing varies from N 16° E to N 110° E depending upon position along the channel. If seismic coverage extended out to outcrop, the trend at outcrop could easily be determined. All that can be attempted here is to assume that the meandering can be described by a regular curve such as a sine wave and predict channel orientation by extrapolation. Channel B,for example, can be fit with a sine wave having a wavelength of 1,100 ft. If we use this figure for all three channels and utilize the ranges to outcrop of 950 ft for C, 1,100 ft for B, and 1,200 ft for A, the following estimates of meander trend at outcrop are derived A - N60°E; B-N80°E; C-N110°E. That is, A and B agree quite well with channels 7 and 10 from the outcrop study while channels C and 8 are in even worse agreement. Channel 8, trending north, is quite anomalous compared to other observed channel trends at this level, although some seismic evidence indicating other than the N 60° E trend exists at other depth levels. The position of channel 8 still is best suited as the interpreted counterpart of seismic channel C, the discrepancy in trend needs to be explained. Possible explanations include: a) channel 8 is actually a different channel which has eroded down through C at this position, b) an error occurred in calculation of the outcrop analysis, c) channel C actually corresponds to another channel, such as number 4 or, d) meanders cannot be described by a simple sine function. It is not likely that this discrepancy can be resolved.

6.0 CONCLUSIONS

Both the cross-sectional appearance of discontinuous events and the meandering nature of these events as they are seen in map view lead to the conclusion that they do represent sandstone channels. The events are discontinuous in a lateral sense only; they do exhibit continuity along their long axes as would be expected. The seismically interpreted shapes of the three channels described are in agreement with the normally observed sandstone

channels in this area. Projection of seismically observed patterns to outcrop encounters real channels at or near the predicted position whose geometries are similar to those predicted. Trend of the channel at outcrop, Comparing seismic prediction with stratigraphic estimation, is less in agreement. However, considering that the seismic estimate is based upon a mathematical extrapolation and that the stratigraphic estimate has some statistical uncertainty, the agreement for all but channel C is quite good. The primary uncertainties found in the seismic data revolve around depicting an accurate geometry (i.e. thickness and width) of individual lenses. Current data processing developments (wavelet extraction, amplitude analysis), together with more detailed model studies might help resolve the thickness variations of these relatively thin beds. Migration of the data would be useful in delineating the width although this is a less confining problem. The main success of this experiment is felt to be in the determination of channel trend; both the azimuthal bearing and the dip. This is important for predicting where subsequent wells might be placed to encounter the same channel and also how the channel trends in relation to the in situ stress field - an important aspect of massive hydraulic fracturing treatment.

7.0 ACKNOWLEDGEMENTS

I would like to acknowledge the contributions of Bill Cashion (U.S.G.S.), Carroll Knutson (C.K. Geoenergy), and Stan Brasel (Seismic International Research) to the planning, execution, interpretation of this project. Funding for this project was provided through the Gas Research Institute and the U. S. Department of Energy.

8.0 REFERENCES

Cashion, William B., 1973, Geologic and structure map of the Grand Junction Quadrangle, Colorado and Utah: Misc. Geol. Invest. Map I-736, U. S. Geol. Survey, Wash., DC.

Dobecki, T. L., 1980, Seismic reflection mapping of discontinuous sandstone bodies - Part I synthetic modeling study: Sandia National Laboratories report SAND80-1455/I, Albuquerque, NM.

Knutson, Carroll F., 1978, Development of techniques for optimizing selection and completion of western light gas sands: Phase I report prepared for the U.S.D.O.E., Nevada Operations Office DOE/BC/10005-1, 49 p.

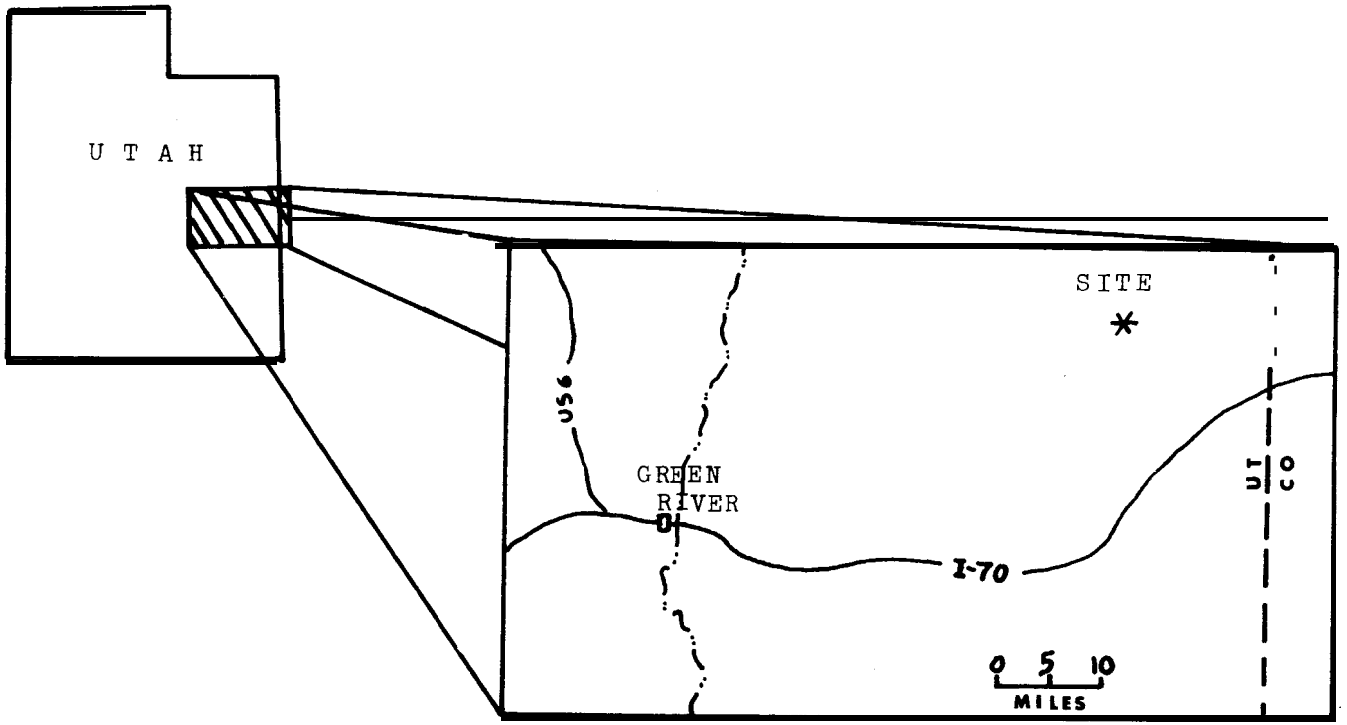

FIG. 1 General location of Bryson Canyon seismic experiment.

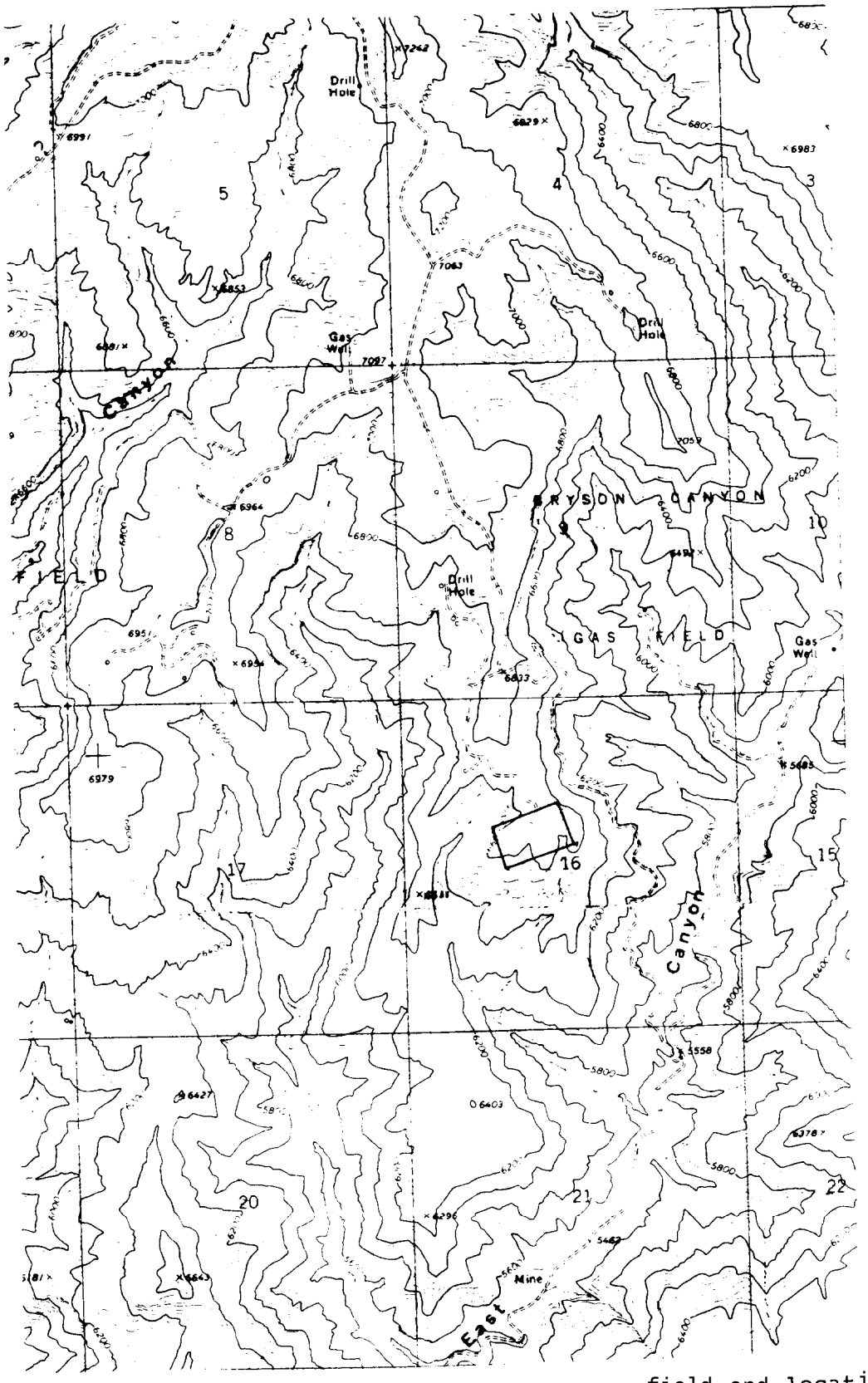

FIG. 2 Topographic map of Bryson Canyon gas field and location of seismic survey. Seismic coverage is within the rectangular area on map.

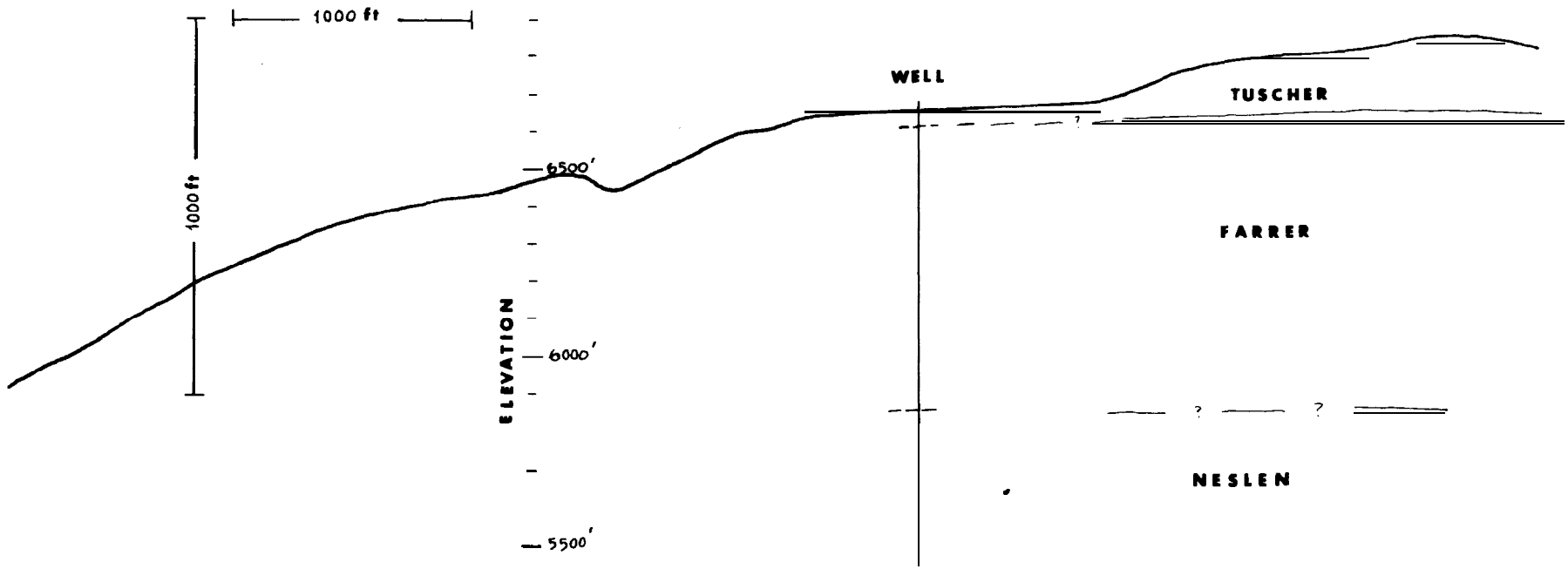

FIG. 3 A generally south to north topographic cross section of the seismic survey area. Depths to formation contacts are valid at the well location. The seismic survey is the flat area around the well location.

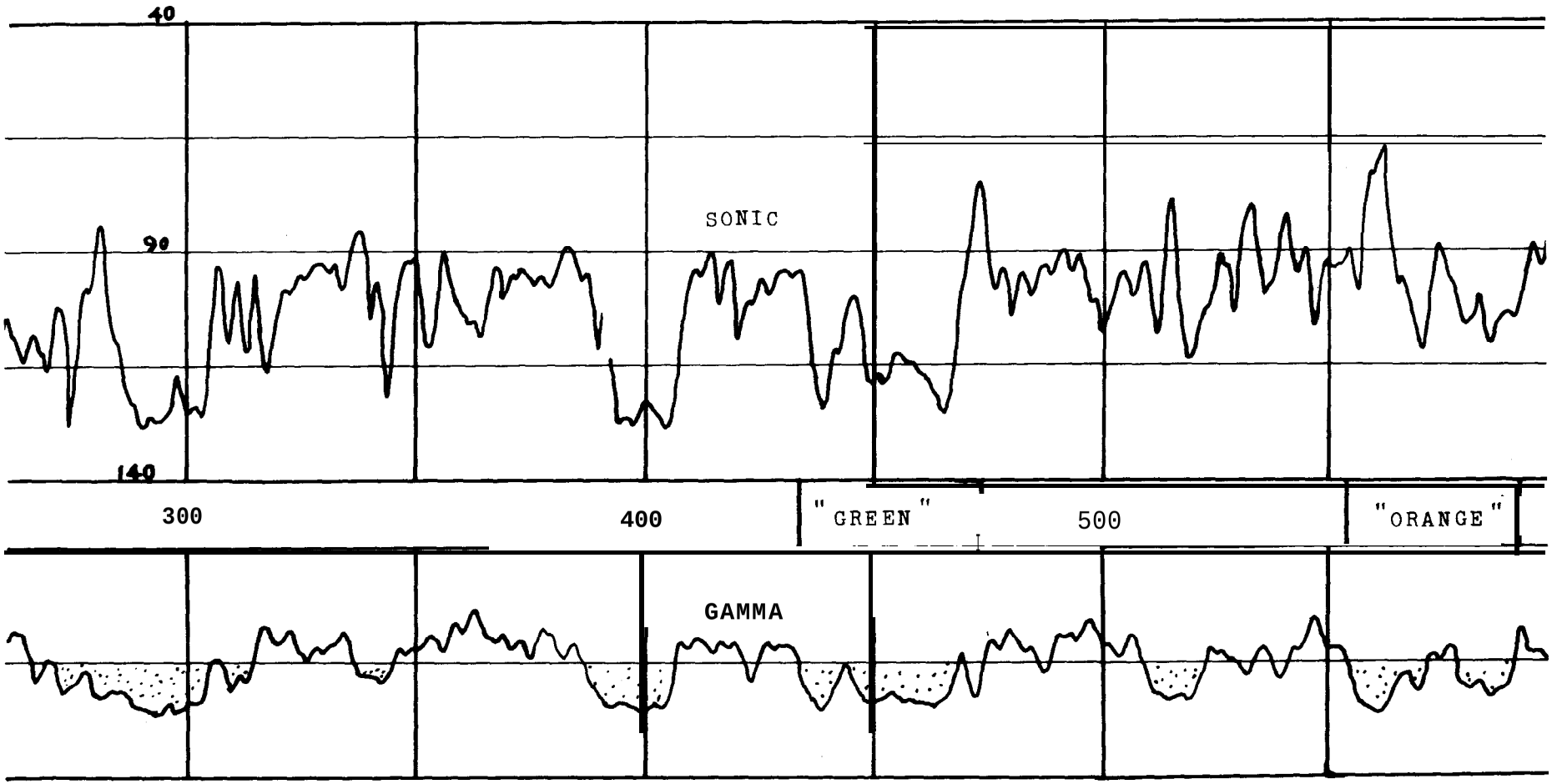

FIG. 4 Segment of BHC sonic log and natural gamma log for corehole GC #1. Interval transit times shown as sonic scale are in microseconds per foot. Note the sand labeled "Green."

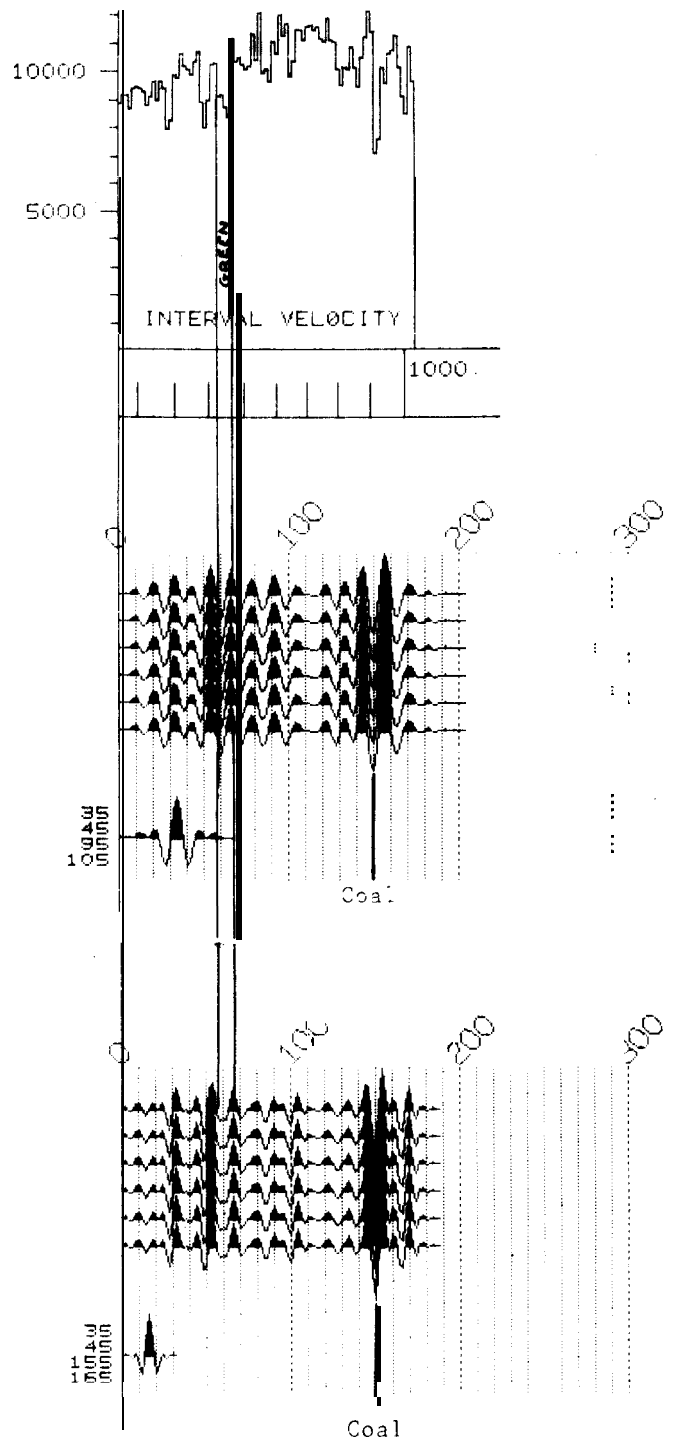

FIG. 5 Synthetic seismogram from sonic log of well GC #1. Two different bandpass wavelets are used. Start depth of the log is 160 ft.

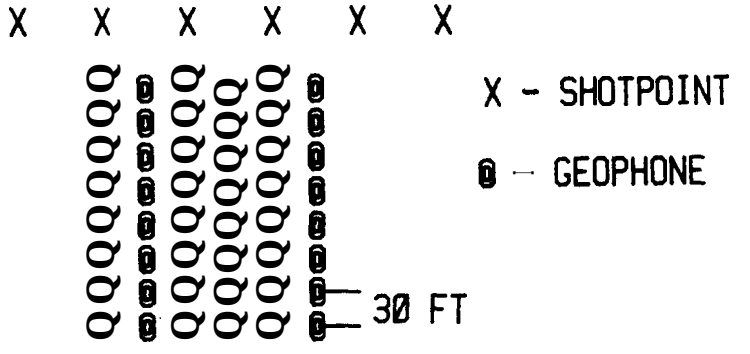

FIG. 6 Shotpoint - geophone array layout as used in acquiring 3-D seismic data.

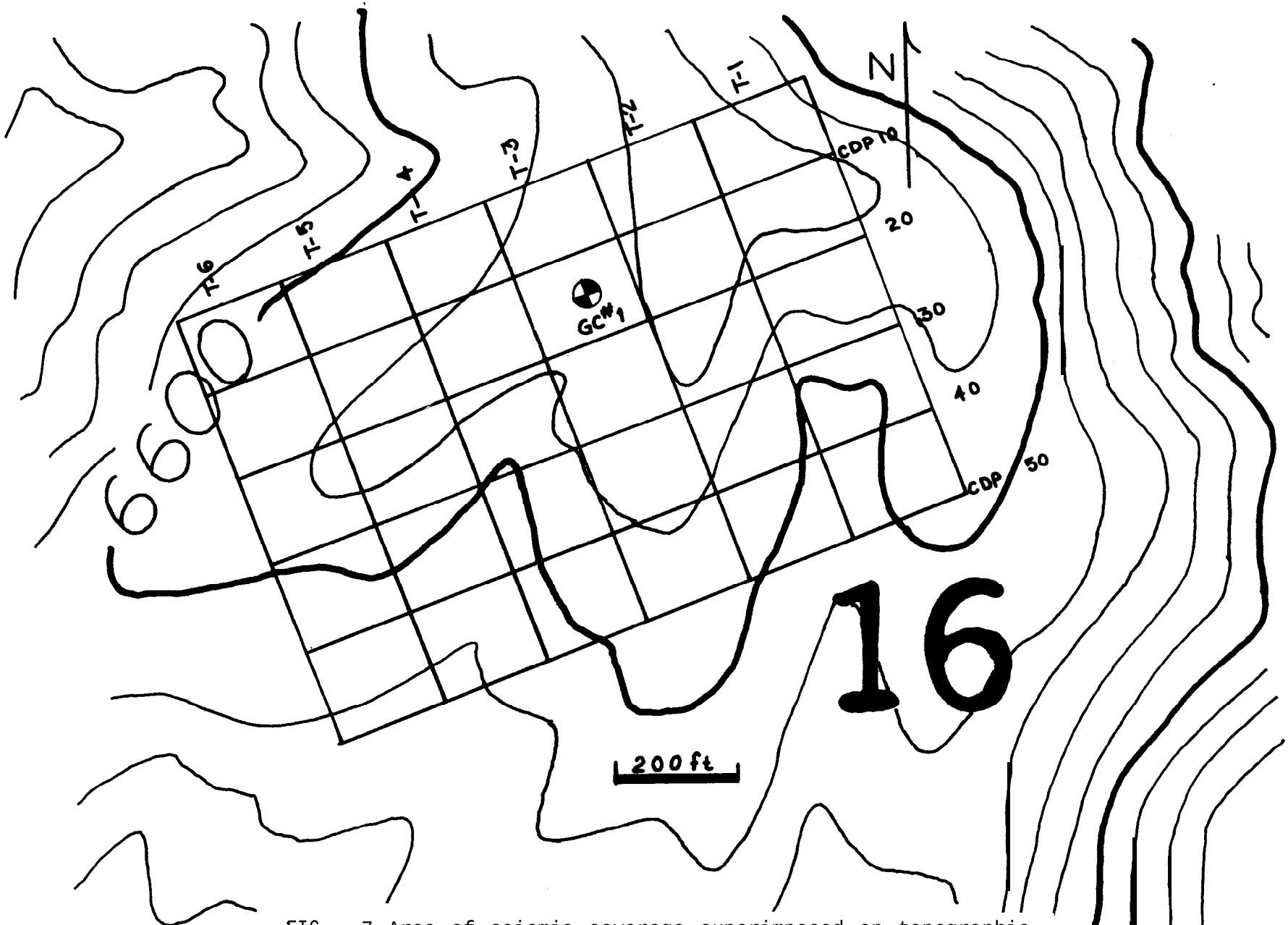

FIG. 7 Area of seismic coverage superimposed on topographic map. Area1 coverage is 750 ft x 1,080 ft; CDP spacing is 15 ft making at 50 x 72 grid of CDP's uniformly covering the area.

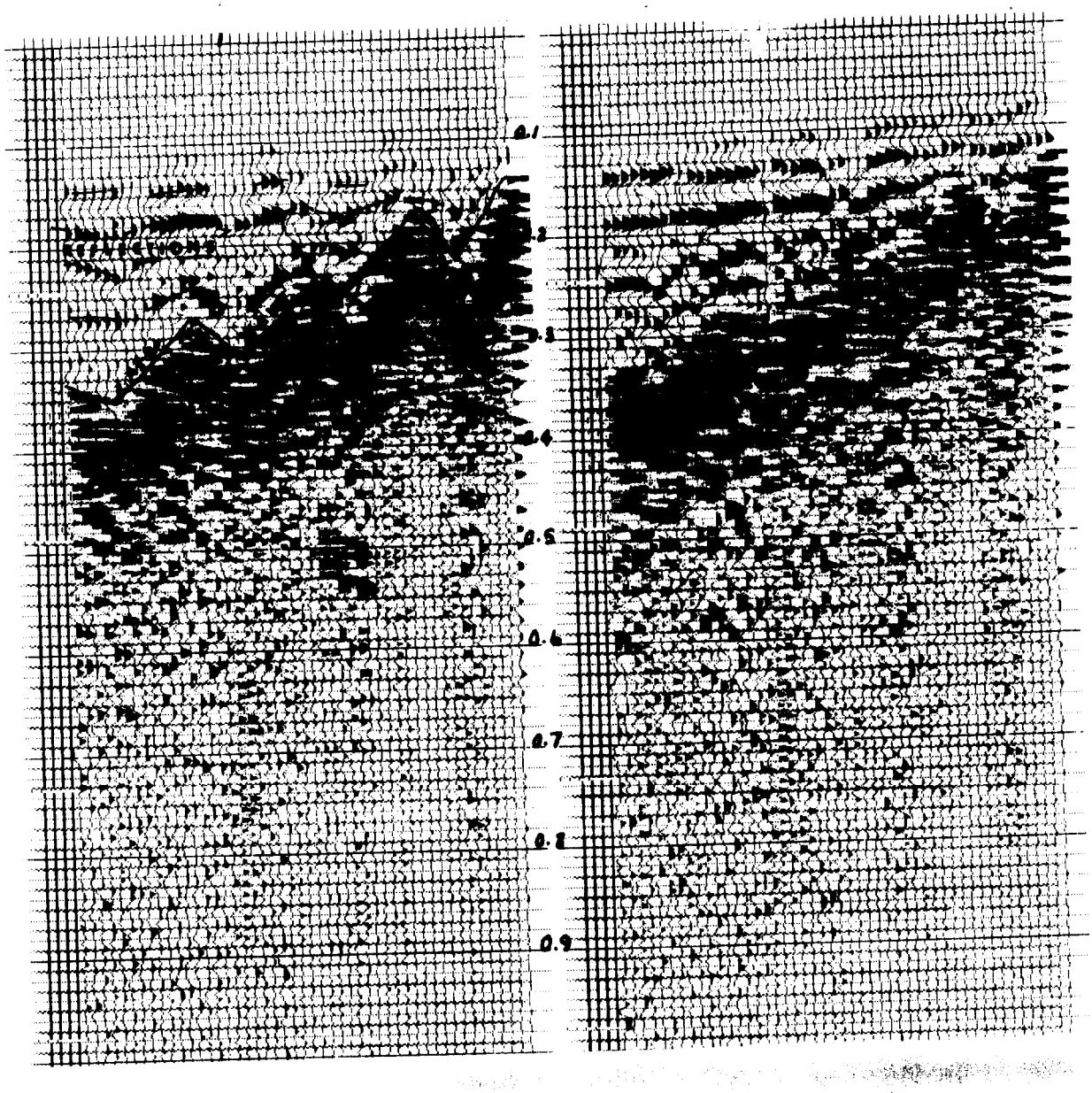

FIG. 8 Raw output of the shot records. Shots are recorded by an 8 x 6 array of recording stations. Vertical scale is travel time in seconds.

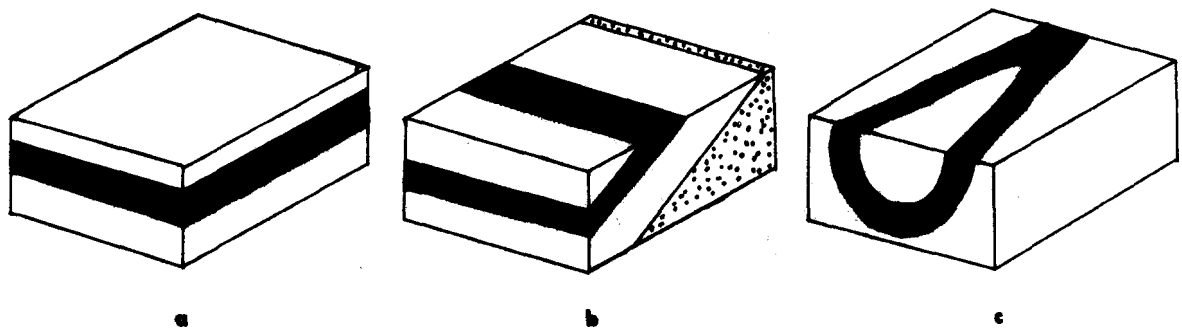

FIG. 9 Perspective view of three 3-D structural situations: a) horizontal planar beds, b) dipping planar beds, and c) dipping folded beds.

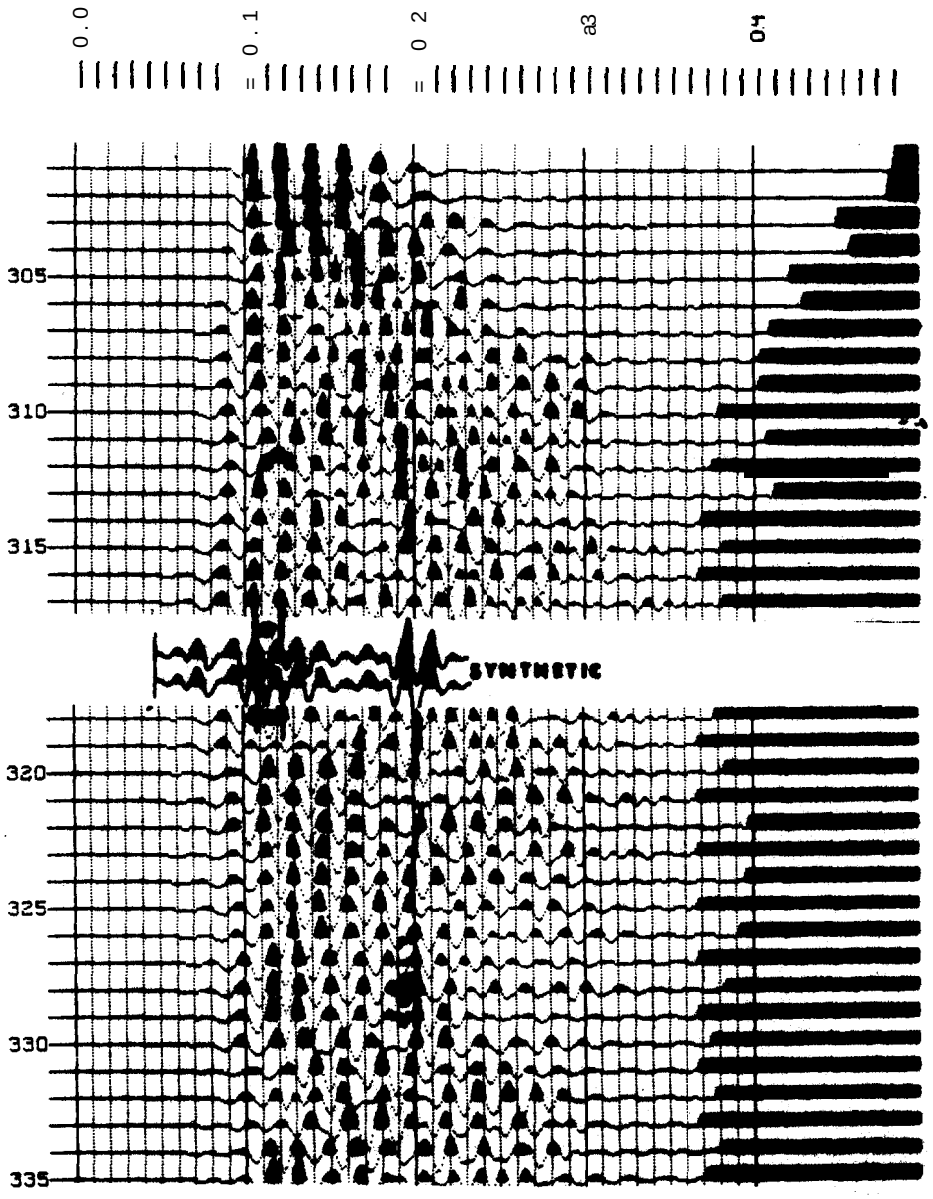

FIG. 10 Part of traverse section 3 together with CG #1 synthetic at approximate location of well.

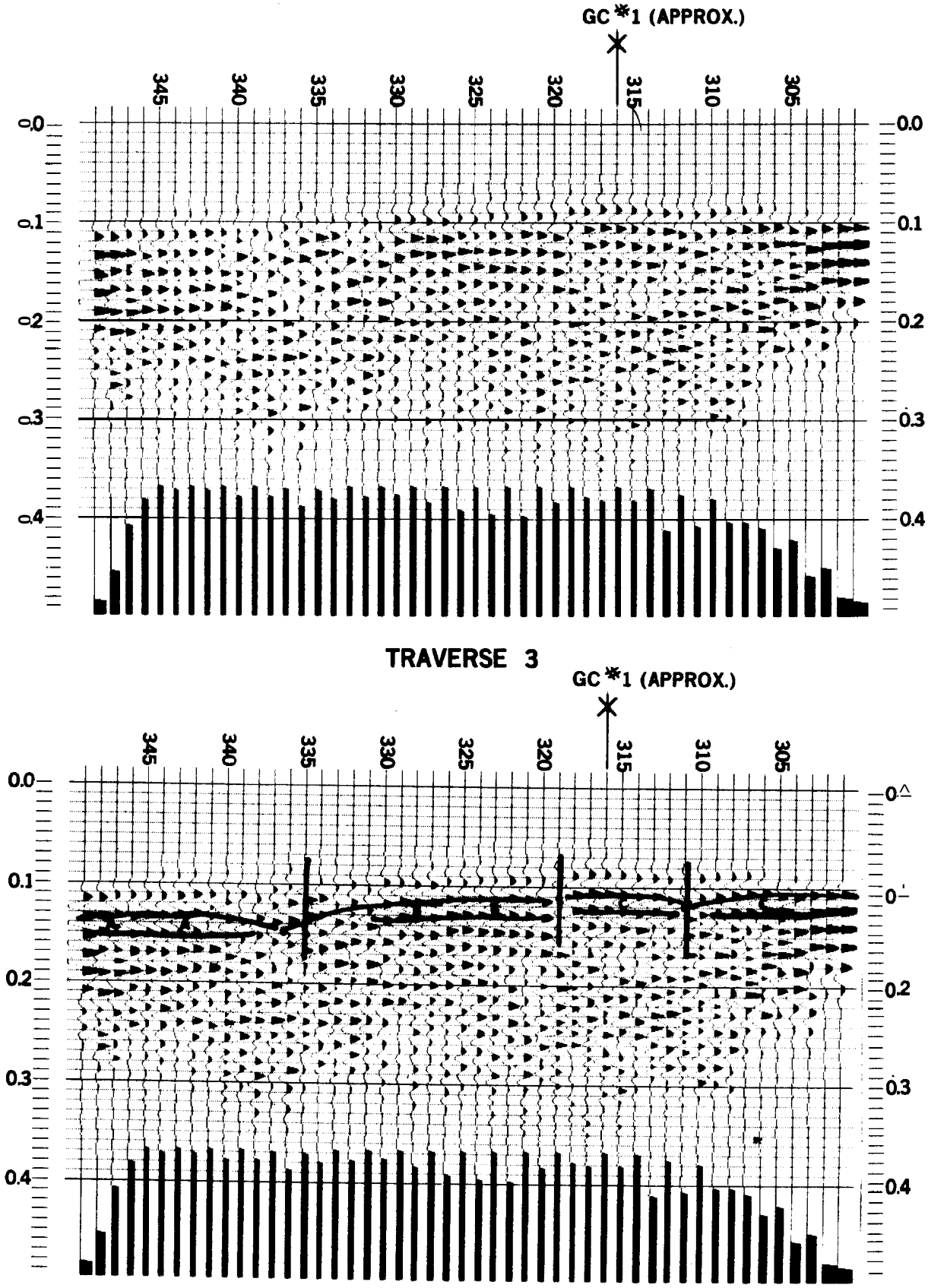

FIG. 11 Two-dimensional seismic section (vertical size) along traverse number 3; a) uninterpreted, b) interpreted.

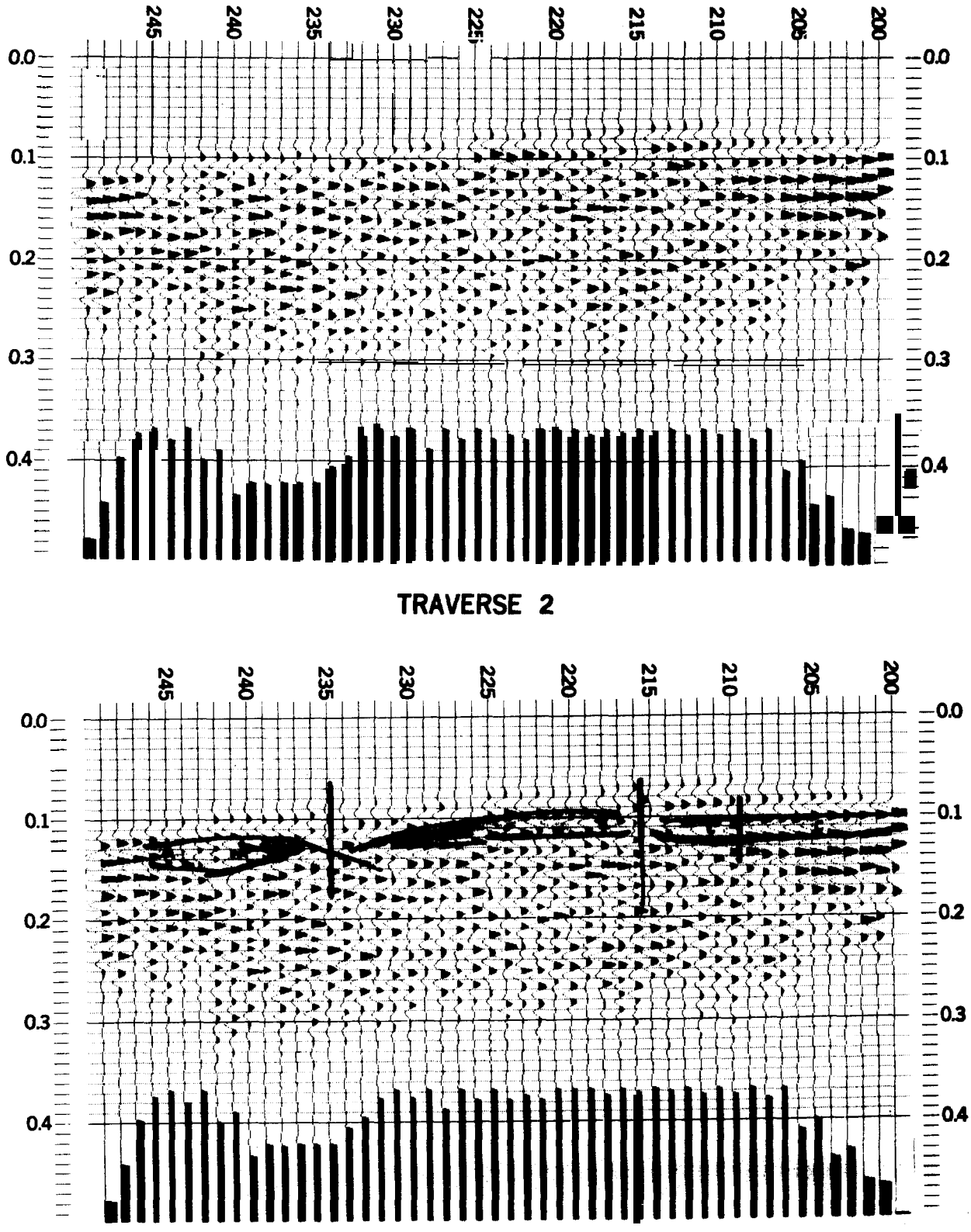

FIG. 12 Traverse 2 seismic section; a) uninterpreted, b) interpreted.

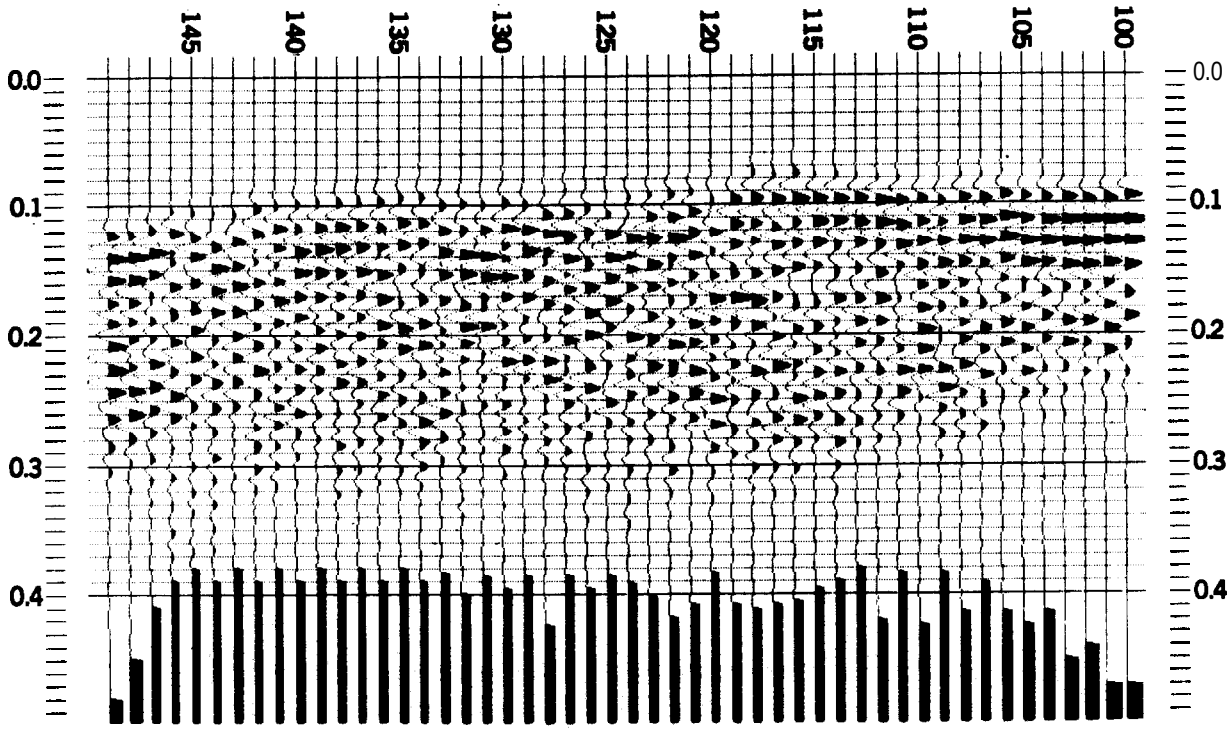

TRAVERSE 1

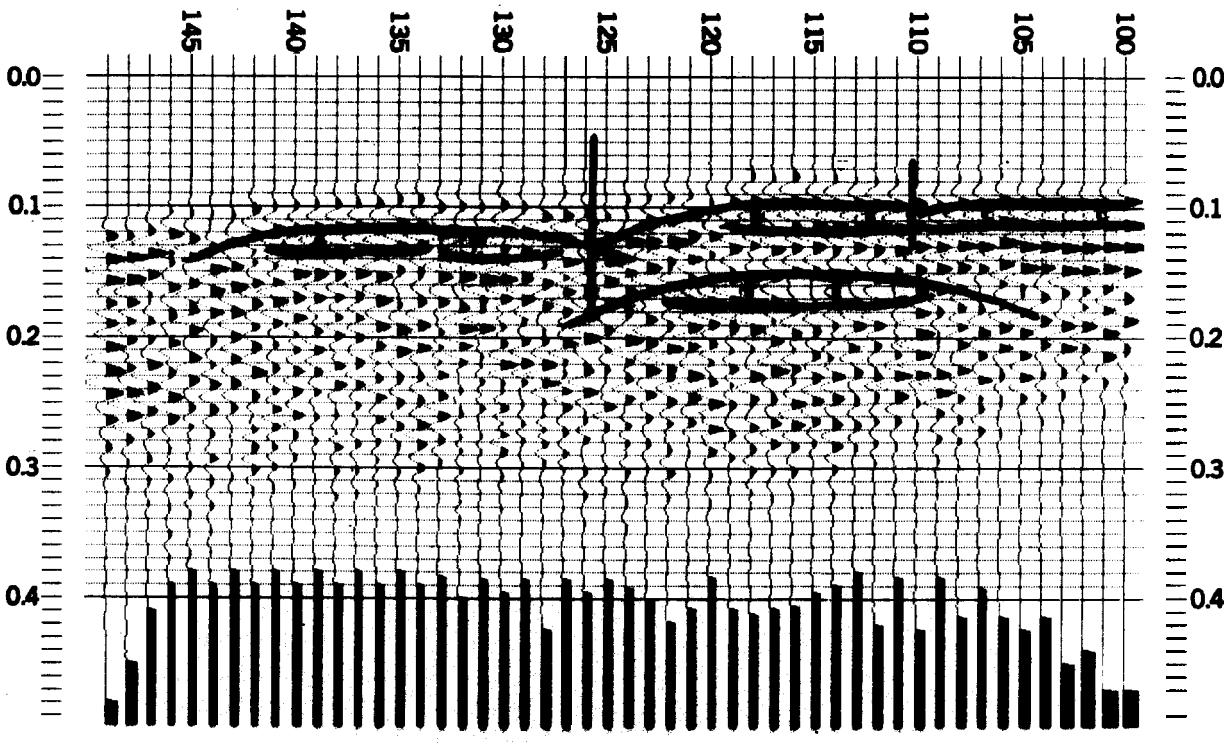

FIG. 13 Traverse 1 seismic section: a) uninterpreted, b) interpreted.

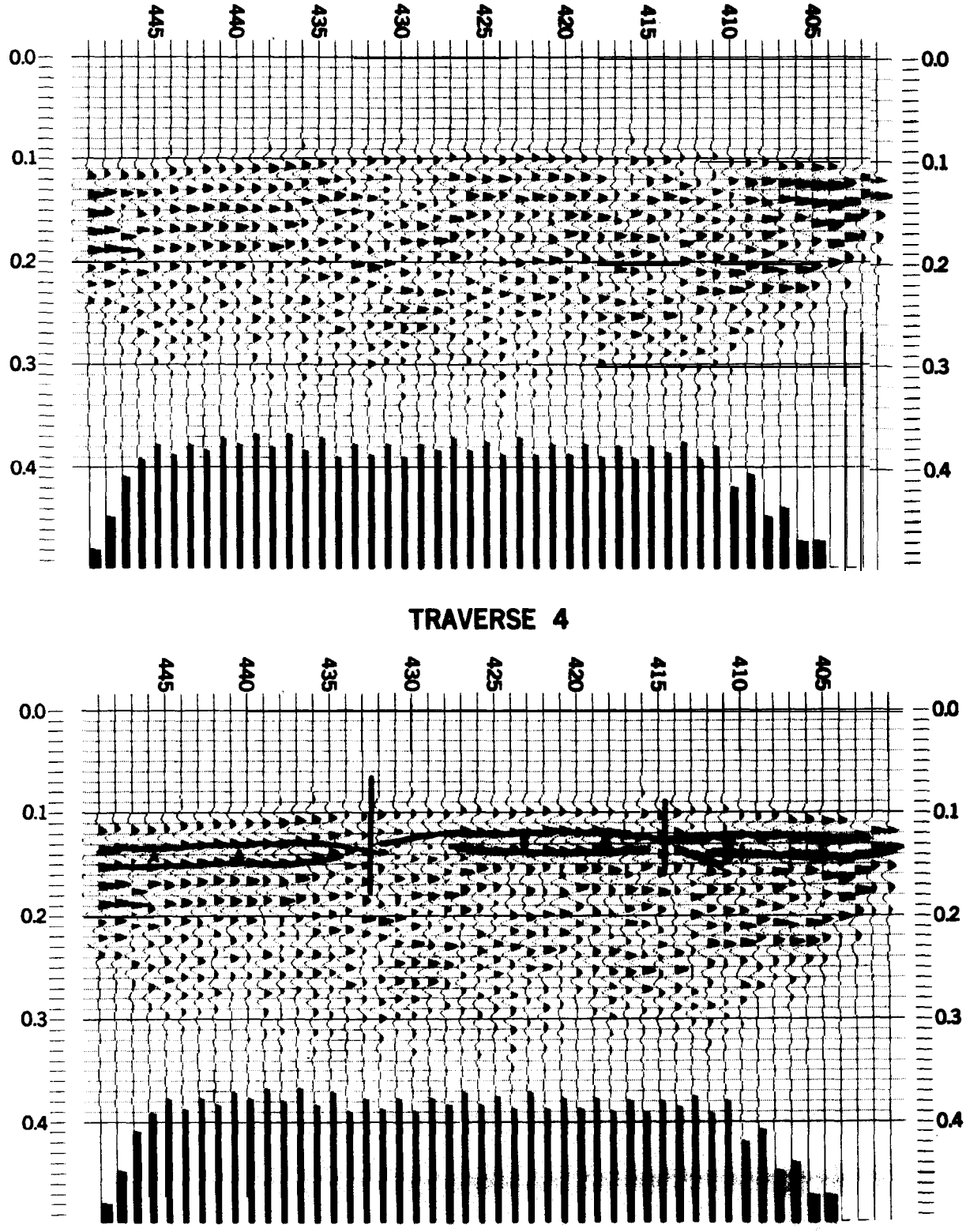

FIG. 14 Traverse 4 seismic section: a) uninterpreted, b) interpreted.

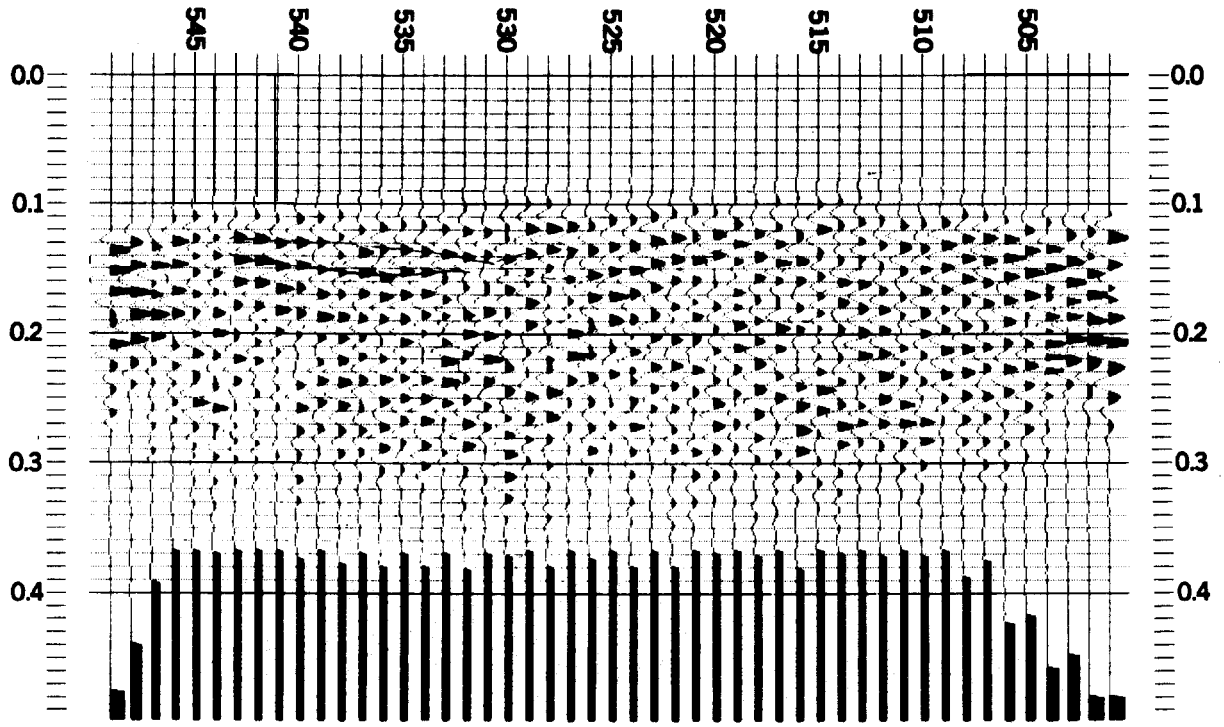

TRAVERSE 5

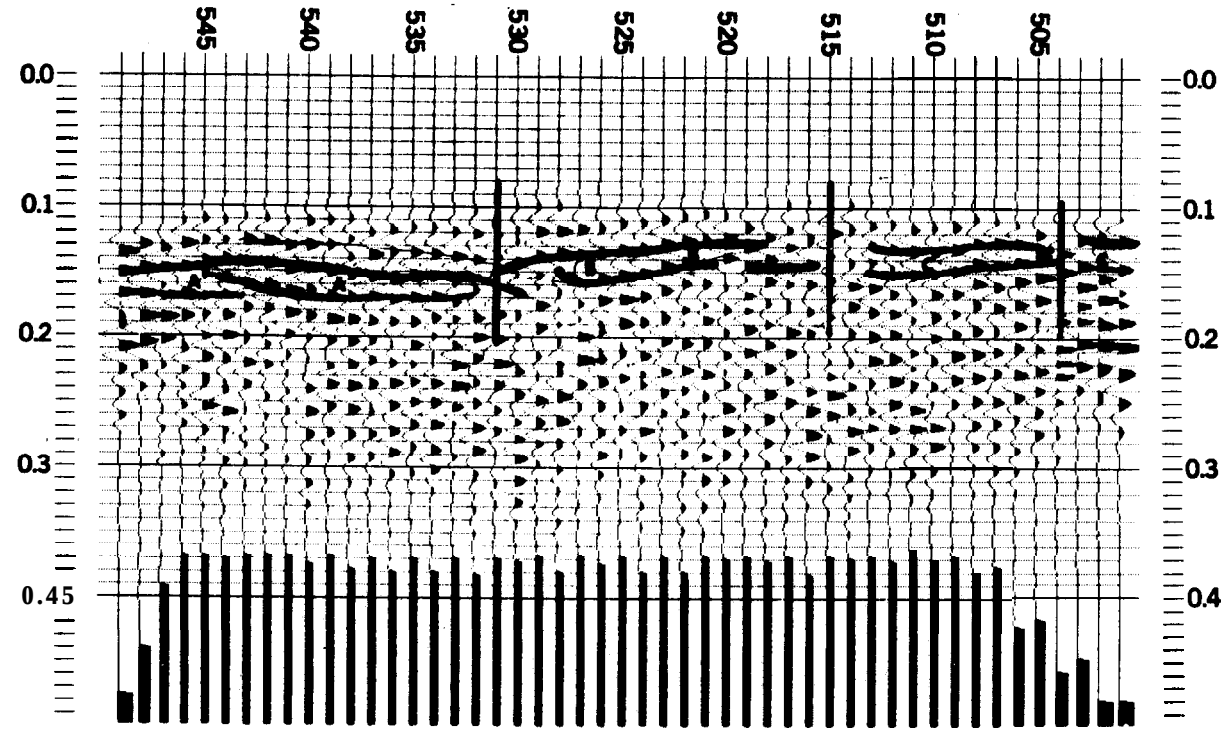

FIG. 15 Traverse 5 seismic section; a) uninterpreted, b) interpreted.

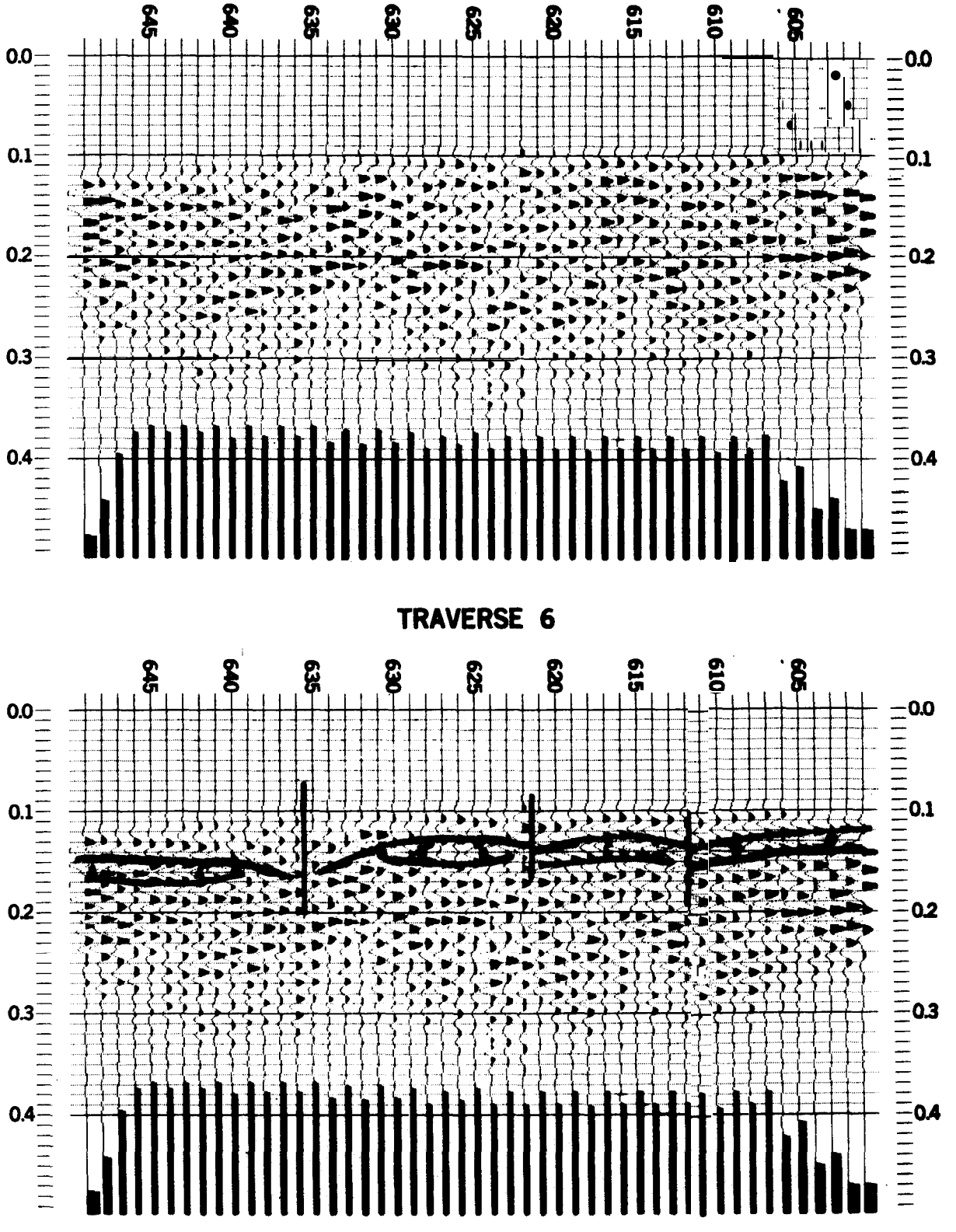

FIG. 16 Traverse 6 seismic section; a) uninterpreted, b) interpreted.

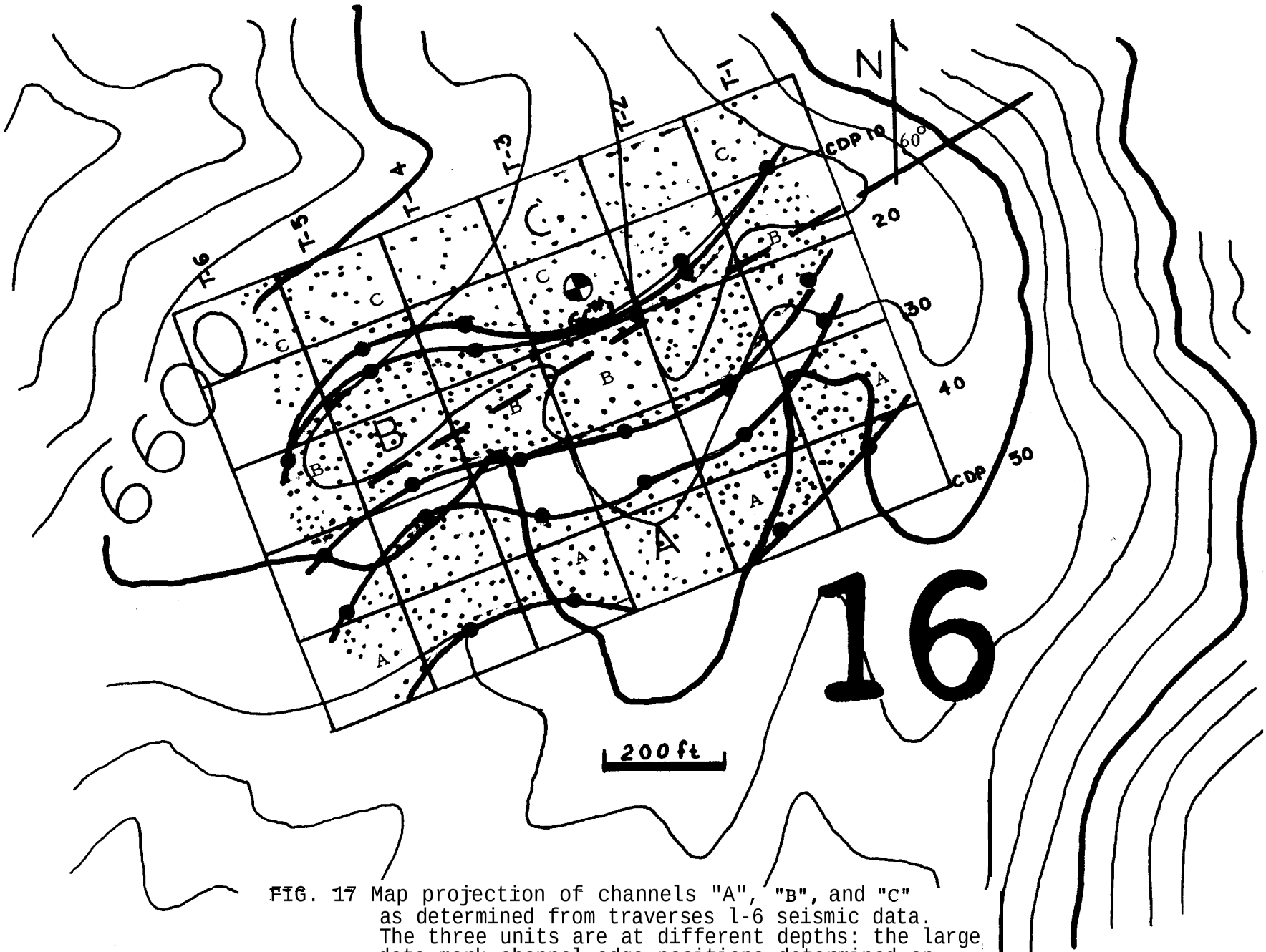

FIG. 17 Map projection of channels "A", "B", and "C" as determined from traverses l-6 seismic data. The three units are at different depths: the large dots mark channel edge positions determined on the sections.

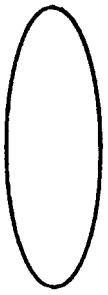

DIP ANGLE = 90

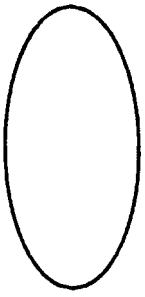

DIP ANGLE = 45

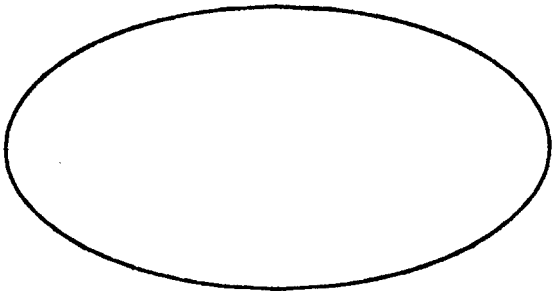

DIP ANGLE = 10

DIP ANGLE = 0

FIG. 18 Horizontal cross-sections, or outcrop patterns, of the same, elliptical channel for four different values of dip. For the 90 degree section, the channel is vertical: for the 0 degree section, the channel is horizontal.

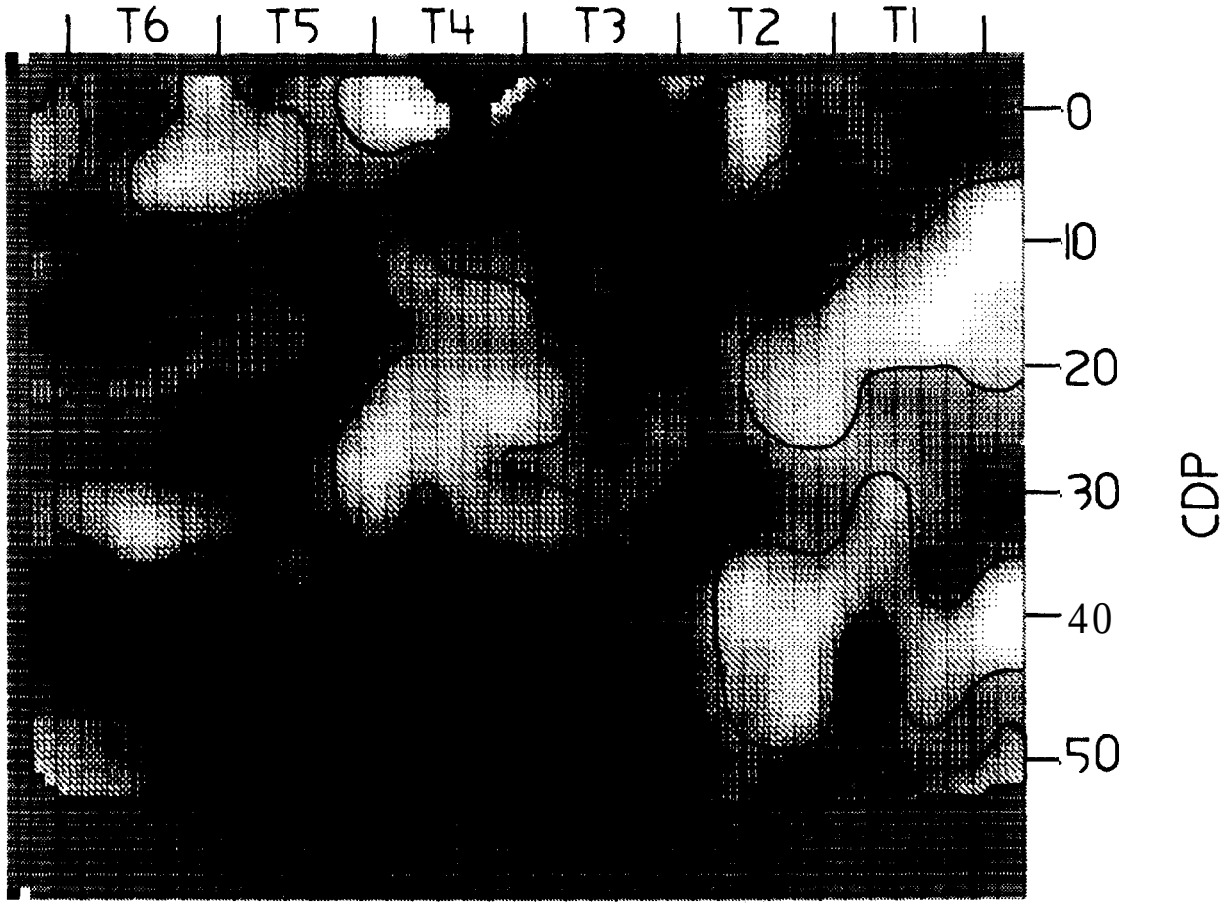

FIG. 19 Example of time slice at T = 0.136 sec. "T" implies traverse number; "CDP" is common depth point number.

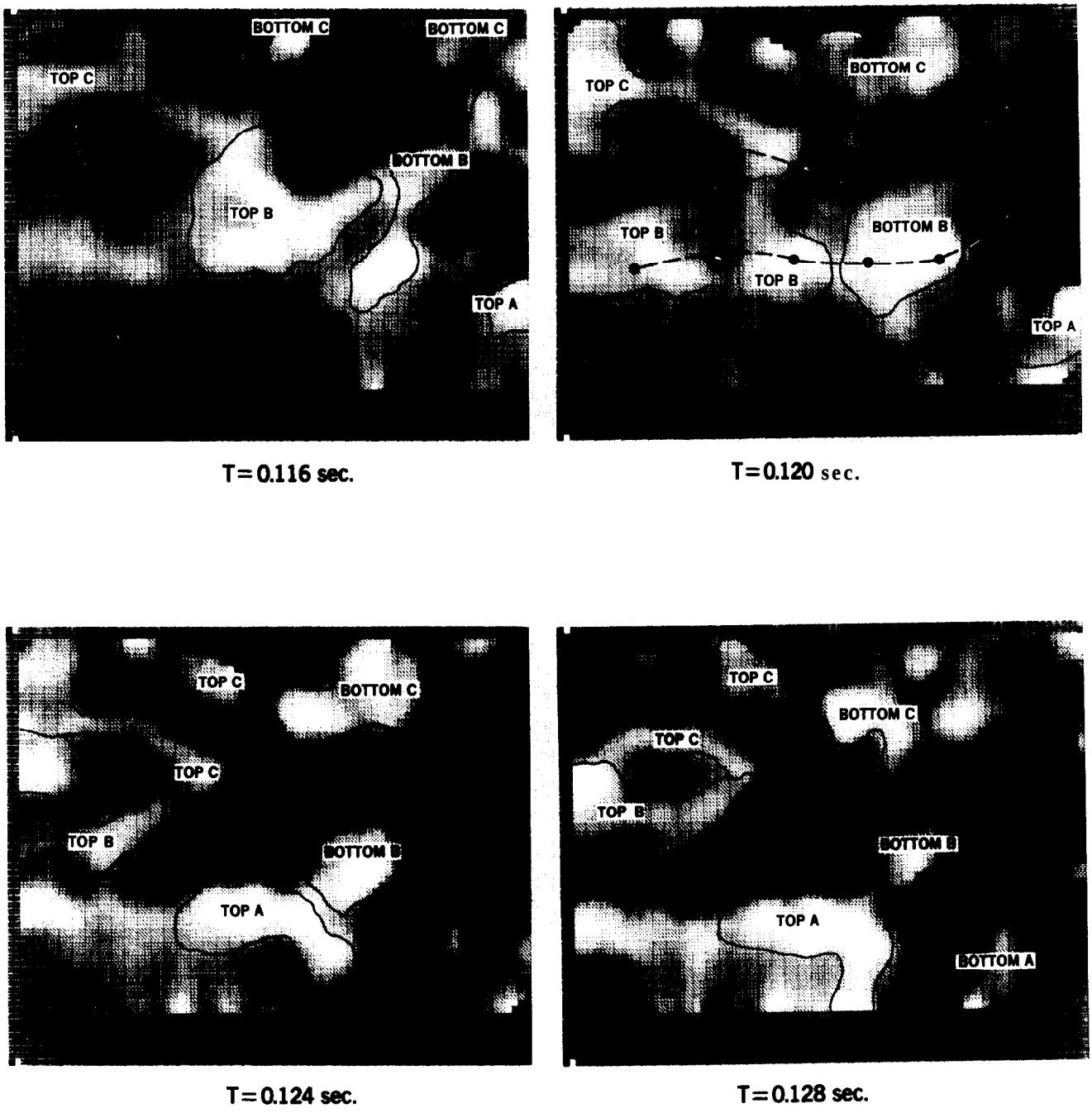

FIG. 20 Interpreted time slices of 3-D seismic data at four millisecond slices. "Top" represents the top peak of the given channel reflection; "Bottom" represents the bottom peak. Superimposed on the 0.120 sec slice is the pattern of channel B from Figure 17.

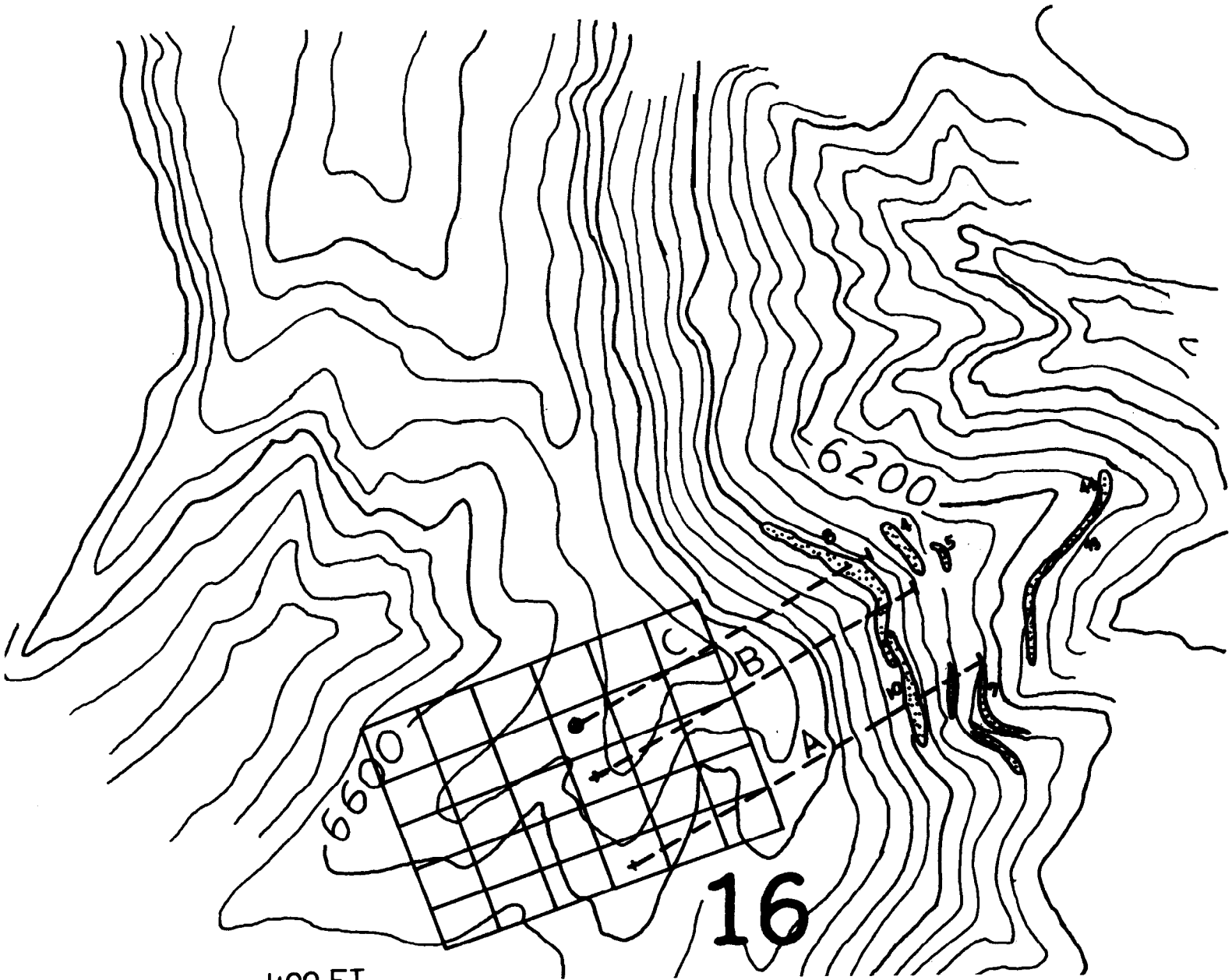

FIG. 21 Map showing projected average trends of channels A, B, and C (dashed lines), their projected outcrop (end of dashed lines), and the positions of mapped outcropping channels in the area (stippled areas).

DISTRIBUTION Cont'd.

Gas Producing Enterprises, Inc.
2100 Prudential Plaza
P. 0. Box 749
Denver, CO 80201
Attn: R. Merrill

Dowel1
P. 0. Box 21
Tulsa, OK 74102
Attn: R. Steanson

Institute of Gas Technology
3424 S. State St.
Chicago, IL 60616
Attn: P. Randolph

Amoco Production Co. (3)
P. 0. Box 591
Tulsa, OK 74102
Attn: R. L. Huggins
R. W. Veatch
M. B. Smith

M. D. Wood, Inc.
1000 Elwell Court
Suite 218
Palo Alto, CA 94303
Attn: M. D. Wood

Gulf Research and Development
Company
P. 0. Drawer 2038
Pittsburgh, PA 15230
Attn: R. P. Trump

Terratek
University Research Park
420 Wakara Way
Salta Lake City, UT 84108
Attn: A. S. Abou-Sayed

Dept. of Engineering Mechanics
Ohio State University
Boyd Laboratory
155 West Woodruff Avenue
Columbus, OH 43210
Attn: Prof. S. H. Advani, Chairman

University of Minnesota
Dept. of Civil and Mineral Eng.
Minneapolis, MN 55455
Attn: Dr. Charles Fairhurst

School of Civil and Environmental
Engineering
Hollister Hall
Cornell University
Ithaca, NY 14853
Attn: Dr. A. R. Ingraffea

U. S. Geological Survey
345 Middlefield Road
Menlo Park, CA 94025
Attn: Dr. D. D. Pollard

Fracturing Technology, Inc.
10301 N. W. Freeway
Suite 202
Houston, TX 77092
Attn: A. R. Sinclair, President

Gas Research Institute
10 West 35th St.
Chicago, IL 60616
Attn: J. C. Sharer

U. S. Geological Survey
Box 25046
Office of Energy Resources
Branch of Oil and Gas Resources
Denver Federal Center
Denver, CO. 80225
Attn: W. B. Cashion

1 M. Sparks
1000 G. A. Fowler
1100 C. D. Broyles
1110 J. D. Kennedy
Attn: C. R. Mehl, 1111
C. W. Smith, 1111
1120 T. L. Pace
1130 H. E. Viney
Attn: B. G. Edwards, 1131
W. C. Vollendord, 1131
3141 T. Werner (5)
3151 W. L. Garner (3)
3154-3 R. P. Campbell
for DOE/TIC (25)
4400 A. W. Snyder
4500 E. H. Beckner
4537 L. D. Tyler
4700 J. H. Scott
4710 G. E. Brandvold
4720 V. L. Dugan
4730 H. M. Stoller
4731 B. Granoff
4732 D. A. Northrop
4733 C. L. Schuster
4734 A. L. Stevens
4737 B. E. Bader
4737 L. C. Bartel
4738 R. L. Fox
4740 R. K. Traeger
5500 0. E. Jones
Attn: W. Herrmann, 5530
4800 R. S. Claassen
8266 E. A. Aas
4739 T. L. Dobecki (15)

DISTRIBUTION:

U. S. Dept. of Energy
MS D-107
Fossil Energy
Washington, DC 20545
Attn: G. Fumich
Assist. Secretary for
Fossil Energy

U. S. Dept. of Energy (4)
Office of Oil and Gas Technology
MS D-107
Washington, DC 20545
Attn: M. Adams
J. W. Watkins
P. R. Wieber
J. B. Smith

U. S. Dept. of Energy
Office of Fossil Energy
Rm. A-117
Washington, DC 20545
Attn: C. W. Guidice
Acting Deputy, Assist.
Secretary for Management

U. S. Dept. of Energy (9)
Morgantown Energy Technology Center
P. 0. Box 880
Morgantown, WV 26505
Attn: A. A. Pitrolo, Director
L. A. Schrider
A. E. Hunt
R. L. Wise (5)
C. A. Komar

U. S. Dept. of Energy
Nevada Operations Office
P. 0. Box 14100
Las Vegas, NV 89114
Attn: C. H. Atkinson

CER Corporation (3)
P. 0. Box 15090
Las Vegas, NV 89114
Attn: G. R. Leutkenhaus
R. L. Mann
E. Evered

U. S. Dept. of Energy (8)
Bartlesville Energy Tech. Center
Bartlesville, 'OK 74003
Attn: R. T. Johansen
D. C. Ward
A. B. Crawley (5)
H. B. Carroll

U. S. Dept. of Energy
Special Programs Division
Albuquerque Operations Office
Albuquerque, NM 87185
Attn: D. L. Krenz, Director

Lawrence Livermore Laboratory
Livermore, CA 94550
Attn: M. E. Hanson

Los Alamos Scientific (3)
Laboratory
Los Alamos, NM 87545
Attn: R. Brownlee, G-Division
W. G. Davey, Q-Division
W. J. Carter, G-7

Halliburton Services (2)
Research Center
Duncan, OK 73533
Attn: A. B. Waters
A. A. Daneshy

Shell Development Company
3737 Bellaire Boulevard
Houston, TX 77001
Attn: R. Saucier

Mobil Research and Development
Corporation
Field Research Laboratory
P. 0. Box 900
Dallas, TX 75211
Attn: J. L. Fitch

Continental Oil Company (2)
Production Research Division
Ponca City, OK 74601
Attn: H. C. Walther
H. Wahl

Columbia Gas System Service (2)
Corporation
1600 Dublin Road
Columbus, OH 43215
Attn: R. Forrest
S. McKetta

Mr. S. D. Brasel
Seismic International Research
1531 stout
Suite 310
Denver, CO 80202

C. K. Geoenergy Corporation
Suite A103
5030 Paradise Road
Las Vegas, NV 89119
Attn: Dr. Carroll F. Knutson